413 APDA-218
(ENDF-122)

MASTER

APDA

EVALUATED NEUTRON CROSS SECTIONS OF PU-240 FOR THE ENDF/B FILE

T. A. Pitterle

M. Yamamoto

JUNE, 1968

ATOMIC POWER
DEVELOPMENT ASSOCIATES, INC.

DISCLAIMER

This report was prepared as an account of work sponsored by an agency of the United States Government. Neither the United States Government nor any agency Thereof, nor any of their employees, makes any warranty, express or implied, or assumes any legal liability or responsibility for the accuracy, completeness, or usefulness of any information, apparatus, product, or process disclosed, or represents that its use would not infringe privately owned rights. Reference herein to any specific commercial product, process, or service by trade name, trademark, manufacturer, or otherwise does not necessarily constitute or imply its endorsement, recommendation, or favoring by the United States Government or any agency thereof. The views and opinions of authors expressed herein do not necessarily state or reflect those of the United States Government or any agency thereof.

DISCLAIMER

Portions of this document may be illegible in electronic image products. Images are produced from the best available original document.

EVALUATED NEUTRON CROSS SECTIONS OF PU-240 FOR THE ENDF/B FILE

T. A. Pitterle

M. Yamamoto*

United States Atomic Energy Commission

Contract No. AT(11-1)-865

Project Agreement No. 18

Approved _____
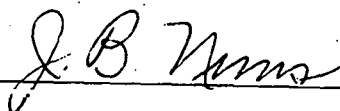
J. B. Nims

Project Engineer

APDA

*Assigned to APDA by
Central Research Institute of Electric Power Industry of Japan

JUNE 1968

THIS PAGE

WAS INTENTIONALLY

LEFT BLANK

SUMMARY

This report describes an evaluation of Pu-240 neutron cross section data carried out for the ENDF/B file. Data were evaluated from 10^{-4} to 15 Mev for the following neutron reactions: total, n-gamma, fission, (n, 2n), (n, 3n), elastic scattering including Legendre polynomial expansions of the angular dependence, nonelastic, and inelastic scattering including resolved levels. Graphs of the evaluated data are included in the report.

THIS PAGE

WAS INTENTIONALLY

LEFT BLANK

TABLE OF CONTENTS

TABLE OF CONTENTS (Continued)

LIST OF ILLUSTRATIONS

LIST OF TABLES

I. INTRODUCTION

In 1966 an evaluation of Pu-240 neutron cross sections was conducted for the ENDF/B file. This report describes the evaluation, which was carried out as part of a cooperative effort by the Cross Section Evaluation Working Group (CSEWG) coordinated through the National Neutron Data Center at Brookhaven National Laboratory under the sponsorship of the U·S. Atomic Energy Commission. References given in the CINDA index (EANDC-66U, July 1, 1966) were considered in this evaluation, as well as a few references as late as October 1966.

In this evaluation, the mass of Pu-240 is taken as 240.1291 amu for a neutron mass of 1.008986. The resolved and unresolved resonance parameters evaluated are discussed in Chapter II (the unresolved parameters were used to estimate the capture and low-energy fission cross sections); the recommended smooth cross sections and elastic scattering angular expansions are discussed in Chapter III; secondary energy distributions for inelastic scattering, fission, (n, 2n), and (n, 3n) are discussed in Chapter IV. Comparisons with other evaluations are considered in Chapter V, along with a discussion of Pu-240 cross section measurements reported since the evaluation was completed.

Graphs of the evaluated data are included in this report and compared with available experimental data. The ENDF/B data file is available through Brookhaven National Laboratory.

This report supersedes the preliminary document, APDA Technical Memorandum No. 43, describing this evaluation.

THIS PAGE

WAS INTENTIONALLY

LEFT BLANK

II. RESONANCE PARAMETERS

Measurements of Pu-240 resonance parameters available at the time of this evaluation included measurements of the neutron widths up to 950 ev. Table I gives a listing of the resonance parameters considered in the evaluation.

A. RESOLVED RESONANCE PARAMETERS

1. Resonance Energies

For the data given in Table I, the average level spacing below 700 ev is about 17 ev; but above 700 ev, the average spacing is about 23 ev, and only a few neutron widths have been measured. Because the probability of missed levels above 700 ev appears to be very large, only levels below 700 ev were selected for the recommended parameters. Each of the recommended resonances has been recognized in at least two different measurements. The recommended energy range for the resolved resonance region is from 10^{-4} to 685 ev.

For the lowest resonance, the BNL-325[1]-recommended energy of 1.056 ev was used in this analysis. Energies selected for the higher energy resonances are approximate averages of the data given in Table I.

2. Neutron Widths

For the 1.056 ev resonance, a value of 2.35 mv is recommended for the neutron width. This value represents slightly heavier weighting of the measurement of Pattendon and Rainey[2] than apparently given in BNL-325. Pattendon's plutonium sample had a Pu-240 isotopic content of 96%, which is considerably greater than most of the other measurements reported in BNL-325. For the 20.44 ev resonance, the BNL-325 value of 2.3 mv was selected based on the data of Table I as well as additional data given in BNL-325.

For the higher energy resonances, the recommended neutron widths represent compromises of the data of Bockhoff[5] and Asghar.[6] At a few resonances (418.5, 465.7, 473.1, and 631.8 ev) no experimental data for the neutron widths have been reported. For these resonances, the neutron widths have been rather arbitrarily estimated by assuming that the reduced neutron widths for these resonances are about one-half of the smallest widths among the measured values in the neighboring energy range. Justification for this procedure is based on the assumption that the neutron widths for these resonances were too small to be resolved in the given experiment.

TABLE I - EXPERIMENTAL DATA FOR RESOLVED RESONANCE PARAMETERS

E_o, ev	Γ_γ, mv	Γ_n, mv	Γ_f, mv	Γ, mv	Misc	Reference
1.056±.002	31±3	2.30±.15	.006	33±3		BNL-325[1]
1.06					$\sigma_o \Gamma_f/\Gamma =30$b	Leonard[3]
1.0575±.001	29.6±4	2.46±.2		32.1±4		Pattendon[2]
20.4±.1		2.3±.2	<2			BNL-325[1]
20.6						Moyer[4]
20.46+0.009	(21.56±3)	3.44+0.09		25±3		Bockhoff[5]
20.42	20.41±4.6	2.053±0.17				Asghar[6]
20.40±0.05	20.8					Byers[7]
38.1±.2		15±2				BNL-325
38.5						Moyer
38.34±0.02	(24.7±3)	18.3±0.7		43±2		Bockhoff
38.26	17.06±3.9	17.79±1.9				Asghar
38.28±0.06	24.6				cap/fiss $=270^{+108}_{-78}$	Byers
41.6		1.9±.5				BNL-325
41.9						Moyer
41.64±0.02	(32.9±2.5)	16.1±0.5		49±2		Bockhoff
41.62	15.36±2.6	16.17±1.5				Asghar
41.61±0.11	34.8					Byers
66.3		45±20				BNL-325
66.8						Moyer
66.66+0.04	(47.0±6.6)	48.0+1.6		95±5		Bockhoff
66.65	22.25±3.4	50.67±3.0				Asghar
66.43±0.11	16.8					Byers
72.4		29±12				BNL-325
72.9						Moyer
72.83±0.04	(22.2±5.7)	21.8±0.7		44±5		Bockhoff
72.8	17.59±2.4	21.27±1.3				Asghar
72.72±0.14	26.5					Byers
90.0±.5		17±6				BNL-325
90.7						Moyer
90.78±0.06	(28.7±6.3)	13.3±0.3		42±6		Bockhoff
90.8	16.89±2.5	10.38±0.6				Asghar
90.7±0.2	33.5					Byers

TABLE I - EXPERIMENTAL DATA FOR RESOLVED RESONANCE PARAMETERS (Continued)

E_o, ev	Γ_γ, mv	Γ_n, mv	Γ_f, mv	Γ, mv	Misc	Reference
92.5+0.06		2.9+0.1				Bockhoff
92.5	12.1+3.3	2.56+0.2				Asghar
92.5+0.2						Byers
104.3+.5		60+30				BNL-325
105.0						Moyer
105.05+0.07	(31.8+7.6)	44.2+1.6		76+6		Bockhoff
105.1	20.95+2.4	44.94+2.1				Asghar
104.9+0.2	25.3					Byers
120.0+1		50+30				BNL-325
121.5						Moyer
121.67+0.06	(35.1+11)	13.9+0.3		49+11		Bockhoff
121.7	18.55+3.1	11.59+0.8				Asghar
121.5+0.3	49.1					Byers
135.4						Moyer
135.2+0.1	(38.2+10)	17.8+0.2		56+10		Bockhoff
135.4	19.93+3.0	15.85+1.0				Asghar
135.3+0.2	41.4					Byers
151.7						Moyer
151.7+0.1	(32.4+16)	13.6+0.1		46+16		Bockhoff
152.0	17.0+6.5	13.2+4.4				Asghar
151.9+0.3	40.3					Byers
162.3						Moyer
162.9+0.1	(43.4+24)	8.6+0.1		52+24		Bockhoff
163.1		8.8+1.0				Asghar
162.7+0.4	57.7					Byers
169.9						Moyer
170.3+0.1	(36.6+22)	13.4+0.3		50+22		Bockhoff
170.5	14.0+6.5	15.0+1.5				Asghar
170.5+0.5	43.9					Byers
185.8						Moyer
186.1+0.2	(41.0+26)	16.0+0.3		57+26		Bockhoff
186.3	15.0+4.5	17.2+2.0				Asghar
186.3+0.5	54.0					Byers

E_o, ev	Γ_γ, mv	Γ_n, mv	Γ_f, mv	Γ, mv	Misc	Reference
199.6±0.2						Bockhoff
239.3±0.1		11.3±0.3				Bockhoff
239.8	15.0±9.5	12.7±2.2				Asghar
241±1						
260.1						Moyer
260.7±0.1						Bockhoff
260.9	18.0±5.5	22.3±2.0				Asghar
262.±2						Byers
286.6						Moyer
287.3±0.1	(64.9±20)	125.1±3.7		190±16		Bockhoff
287.9	25.0±5.5	130				Asghar
289±2	64					Byers
305.1±0.1		7.0±0.4				Bockhoff
305.8	(20)	6.9±2.0				Asghar
305±1						Byers
315.5						Moyer
318.5±0.1						Bockhoff
320.9±0.1	(77.4±20)	18.6±0.4		96±20		Bockhoff
321.7	(20)	14.4±2.5				Asghar
320±1						Byers
338.7±0.1		5.7±0.4				Bockhoff
338±1						Byers
346.2±0.1	(50.8±27)	16.2±0.4		67±27		Bockhoff
347.2	(20)	14.7±4.3				Asghar
346±1						Byers
364.0±0.1	(43.1±23)	30.9±0.4		74±23		Bockhoff
365.0	(20)	30.0±3				Asghar
364±1						Byers
372.3±0.1		13.3±0.4				Bockhoff
373.2	(20)	12.0±3				Asghar
372±1						Byers

E_o, ev	Γ_γ, mv	Γ_n, mv	Γ_f, mv	Γ, mv	Misc	Reference
404.4						Moyer
405±0.1	(70.5±20.6)	102.5±1.6		173±19		Bockhoff
406	(20)	102±8				Asghar
405±1						Byers
419.0±0.1						Bockhoff
418±.1						Byers
450±0.2	(102±57)	16.8±0.9		119±56		Bockhoff
451	(20)	11±7				Asghar
448±1						Byers
466.4±0.2						Bockhoff
465±1						Byers
473.2±0.2						Bockhoff
473±1						Byers
494.2±0.2		5.1±0.4				Bockhoff
493±1						Byers
499.6±0.2		18.6±0.7				Bockhoff
501	(20)	24±10				Asghar
500±1						Byers
514.6		20.4±0.9				Bockhoff
516	(20)	28±10				Asghar
511±2						Byers
526	(20)	10±10				Asghar
546.8±0.2		29.9±0.7				Bockhoff
549	(20)	35±13				Asghar
546±2						Byers
553.5±0.2		16.7±0.7				Bockhoff
555	(20)	25±14				Asghar
552±2						Byers
566.6±0.2		30.0±0.7				Bockhoff
569	(20)	25±13				Asghar
566±2						Byers

7

E_o, cv	Γ_γ, mv	Γ_n, mv	Γ_f, mv	Γ, mv	Misc	Reference
597.2±0.2		53.0±1.0				Bockhoff
599	(20)	46±16				Asghar
597±2						Byers
608.4±0.2		20.5±1.2				Bockhoff
610	(20)	15±15				Asghar
608±2						Byers
632.6±0.2		12.3±1.0				Bockhoff
631±2						Byers
637.8±0.2						Bockhoff
638±2						Byers
663.9						Moyer
665.5±0.3		183±3				Bockhoff
668	(20)	195±25				Asghar
665±3						Byers
678.9		24.0±1.0		279±40		Bockhoff
681	(20)	26±25				Asghar
678±3						Byers
750.5±0.3						Bockhoff
753	(20)	70±25				Asghar
749±3						Byers
759.6±0.3						Bockhoff
791.4±0.3						Bockhoff
790±4						Byers
811.0±0.3						Bockhoff
814	(20)	210±40				Asghar
810±4						Byers
820.4±0.3						Bockhoff
824	(20)	105±30				Asghar
821±4						Byers
855.4±0.3						Bockhoff
853±4						Byers

TABLE I - EXPERIMENTAL DATA FOR RESOLVED
RESONANCE PARAMETERS (Continued)

E_0, ev	Γ_γ, mv	Γ_n, mv	Γ_f, mv	Γ, mv	Misc	Reference
876.9±0.4						Bockhoff
876±5						Byers
891.8±0.4						Bockhoff
895	(20)	100±46				Asghar
891±5						Byers
904.1±0.4						Bockhoff
909.5±0.4						Bockhoff
907±5						Byers
915.5±0.5						Bockhoff
914	(20)	65±42				Asghar
944.0±0.4						Bockhoff
949	(20)	112±50				Asghar
945±2						Byers
958.8±0.4						Bockhoff
958±5						Byers
971.6±0.4						Bockhoff
972±5						Byers
1002.4±0.4						Bockhoff
1004±5						Byers

All resolved resonances are assumed to be s-wave resonances in this analysis.

3. Radiation Widths

Probably the most important uncertainty in estimating Pu-240 cross sections for fast reactor analysis is due to the discrepancy in measured radiation widths. The measurements considered in this evaluation have not satisfactorily reduced this uncertainty.

Bockhoff et al[5] applied shape and area analysis to transmission experiments to obtain total and neutron widths from which estimates of the radiation width were extracted. The neutron widths are more reliable than

the total widths. Errors applied to the radiation widths for these date in Table I represent the Bockhoff uncertainty for the total and neutron widths. Up to the 105 ev resonance, the uncertainties are less than about 20% of the estimated radiation width; above this energy, the uncertainties are considerably larger.

Asghar et al[6] used area analysis of transmission, capture gamma-ray yield, and scattering yield data to obtain the neutron widths and the radiation widths (16 resonances) given in Table I. Below 140 ev, two sample thicknesses were used for each type of measurement; while above 140 ev, scattering data were not used in the analysis.

The radiation widths given in Table I for the data of Byers et al[7] represent very preliminary estimates privately communicated to the authors of this evaluation to assist in establishing the magnitude of the radiation width. The parameters of Bockhoff[5] were assumed in the analysis of their data (nuclear detonation). Uncertainties in the radiation widths have not been estimated, although they are likely to be of the same order as given for the Bockhoff data.

Other measurements of the radiation width for the 1.056 ev resonance are: Pattendon,[2] 29.6±4; Cote,[8] 32.1±3; and Egelstaff,[9] 38±3.

Average values of the radiation width over two energy intervals are given in Table II. The data of Bockhoff and Byers are consistent except for the 66 ev resonance, which was not included in the averages of Table II. Asghar's average of 18.1 mv is outside the probable uncertainty of the Bockhoff and Byers data. For this evaluation, the average radiation width is taken to be 30 mv, based largely on the Bockhoff[5] data and on the Pattendon[2] and Cote[8] measurements of the 1.056 ev resonance.

For the 1.056 ev resonance, the BNL-325 value of 31 mv for the radiation width was used for this evaluation. Where measurements by Bockhoff and Byers exist, the recommended values are a compromise between the two measurements. For all other resonances, the average value of 30 mv was used for the radiation width.

4. Fission Widths

For the 1.056 ev resonance, the fission width is based on Leonard's[3] value for the peak fission cross section and the recommended parameters for the neutron and radiation widths. The 38.1 ev resonance fission width was obtained from Byers'[7] reported capture/fission ratio of 270 and the recommended capture width of 24.6 mv. An estimate of the fission width for the 20.44 ev resonance was obtained by comparing peak capture and fission cross sections given in the graph of Byers for the 20.44 and 38.1 ev

TABLE II - AVERAGE EXPERIMENTAL RESONANCE PARAMETERS

	BNL-325[1]	Bockhoff[5]	Asghar[6]	Byers[7]
$\langle D \rangle$ ev				
0 - 310 ev	17.9	15.8	16.8	16.7
310 ev - 700 ev		16.3	23.4	17.0
$\langle \Gamma_n^o \rangle, \langle S^{\ell=o} \rangle$				
0 - 450 ev				
$\langle \Gamma_n^o \rangle$ (mv)$^{1/2}$		2.0 (23 res)	2.0 (23 res)	
$\langle S^{\ell=o} \rangle \times 10^4$ (ev)$^{-1/2}$		1.06	1.07	
450 ev - E_{max}				
$\langle \Gamma_n^o \rangle$ (mv)$^{1/2}$		1.52 (11 res)	2.5 (16 res)	
$\langle S^{\ell=o} \rangle \times 10^4$ (ev)$^{-1/2}$		0.728	0.806	
0 - E_{max}				
$\langle \Gamma_n^o \rangle$ (mv)$^{1/2}$ Γ_n^o (mv)$^{1/2}$		1.83	2.20	
$\langle S^{\ell=o} \rangle \times 10^4$ (ev)$^{-1/2}$		0.945	0.929	
$\langle \Gamma\gamma \rangle$, mv				
0 - 106 ev		27.0	17.1	27.6
0 - 300 ev		32.6	18.1	35.5

* Maximum resonance energies for which the resonance parameters were resolved. E_{max} is 679.2 ev for Bockhoff's data; 946 ev for Asghar's data.

resonances. Above the 38.1 ev resonance, the fission cross section is given as a smooth cross section up to the lower energy limit of the unresolved energy range.

5. Recommended Parameters

The recommended resolved resonance parameters are given in Table III. The potential scattering cross section was taken as 10.6 barns, the recommended value for U-238 in ENDF/B. Table IV gives a comparison between measured and calculated values for the resolved resonance integral (including 1/v contribution of 110 barns) and 0.0253 capture cross section. An average of the last four measured values in Table IV for the capture cross section yields a value of 280 barns, in good agreement with the cal-

TABLE III — RECOMMENDED RESOLVED RESONANCE PARAMETERS

E_0, ev	Γ_γ, mv	Γ_n, mv	Γ_f, mv
1.056	31.0	2.35	0.0057
20.44	21.0	2.3	0.182
38.31	24.6	18.05	0.091
41.65	34.0	16.14	0
66.59	30.0	49.34	0
72.75	25.0	21.54	0
90.70	31.0	11.84	0
92.50	30.0	2.73	0
104.9	28.5	44.59	0
121.5	40.0	12.75	0
135.3	39.0	16.83	0
151.8	36.0	13.4	0
162.8	48.0	8.7	0
170.2	39.0	14.2	0
186.1	46.0	16.6	0
240.0	30.0	12.0	0
260.9	30.0	22.3	0
287.9	64.0	127.6	0
305.3	30.0	6.95	0
320.9	30.0	16.5	0
338.4	30.0	5.7	0
346.3	30.0	15.45	0
364.3	30.0	30.45	0
372.5	30.0	12.35	0
405.3	30.0	102.25	0
418.5	30.0	2.45	0
449.7	30.0	13.9	0
465.7	30.0	2.59	0
473.1	30.0	2.61	0
493.6	30.0	5.1	0
500.2	30.0	21.3	0
513.5	30.0	24.2	0
547.3	30.0	33.0	0
553.5	30.0	20.9	0
567.2	30.0	27.5	0
597.7	30.0	49.5	0
608.8	30.0	17.75	0
631.8	30.0	12.3	0
637.9	30.0	3.03	0
666.2	30.0	189.0	0
679.2	30.0	25.0	0

TABLE IV - RESONANCE INTEGRALS AND THERMAL CAPTURE CROSS SECTIONS

Reference	Cutoff Energy, ev	Resonance Integral, barns	0.0253 ev Cross Section
Cornish-1957[10]	0.5	8700 ± 800	250 ± 35
Eroziellinsky-1957[11]		9000 ± 3000	
Kriepchinsky-1957[12]	0.2	10000 ± 2800	
Rose-1958[13]		11300 ± 1000	370 ± 40
Walker-1960[14]	0.5	8780 ± 550	
Nichols-1963[15]	0.6	8607 ± 700	
Walker-1957[16]			335 ± 35
Egelstaff-1957[17]			250 ± 200
Halperin-1958[18]			285 ± 15
Westcott-1959[19]			270 ± 17
Pattendon-1959[2]			273 ± 8
Tattersall-1962[20]	0.5	8380 ± 1100	290 ± 9
Calculated from	0.414	8210	276
recommended parameters	0.500	8160	

culated value of 276 barns. Calculated values for the 0.0253 ev scattering and fission cross sections are 2.08 and 0.053 barns, respectively.

Calculated cross sections from 10^{-3} to 28 ev are shown in Figures 1 through 6. Figure 7 gives half-lethargy group averages of the calculated cross sections up to the upper energy limit of 685 ev for the resolved resonance region. All cross sections from 10^{-3} to 685 ev except the fission cross section between 45 and 685 ev are to be calculated from the resolved parameters, and smooth data are not given in the ENDF/B data.

Below the 1.056 ev resonance, the total cross section is in good agreement with the measurements of Pattendon and Rainey.[2] Between the first three resonances, measured values of the total cross section[2,22] are two to three times greater than the calculated cross section. No attempt has been made in this evaluation to fit the experimental data between resonances with a smooth background cross section, since experimental corrections for sample impurities lead to large uncertainties in the data.

B. UNRESOLVED RESONANCE PARAMETERS

The unresolved energy range has been selected as 685 ev to 40 kev and includes both s- and p-wave contributions. In this section, the selection of the unresolved parameters is discussed.
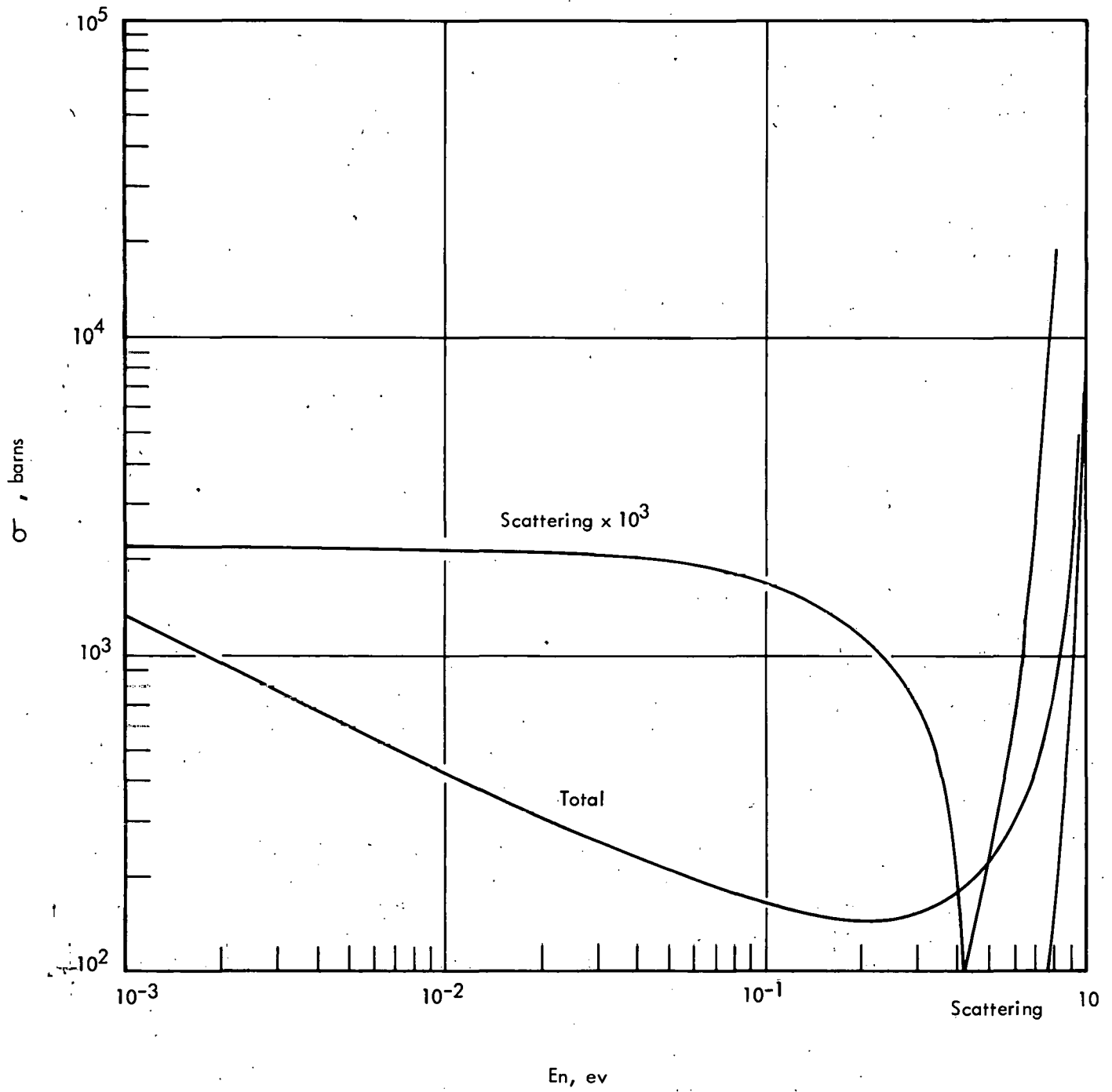
FIG. 1 SCATTERING AND TOTAL CROSS SECTIONS, 10⁻³ EV TO 1 EV

14
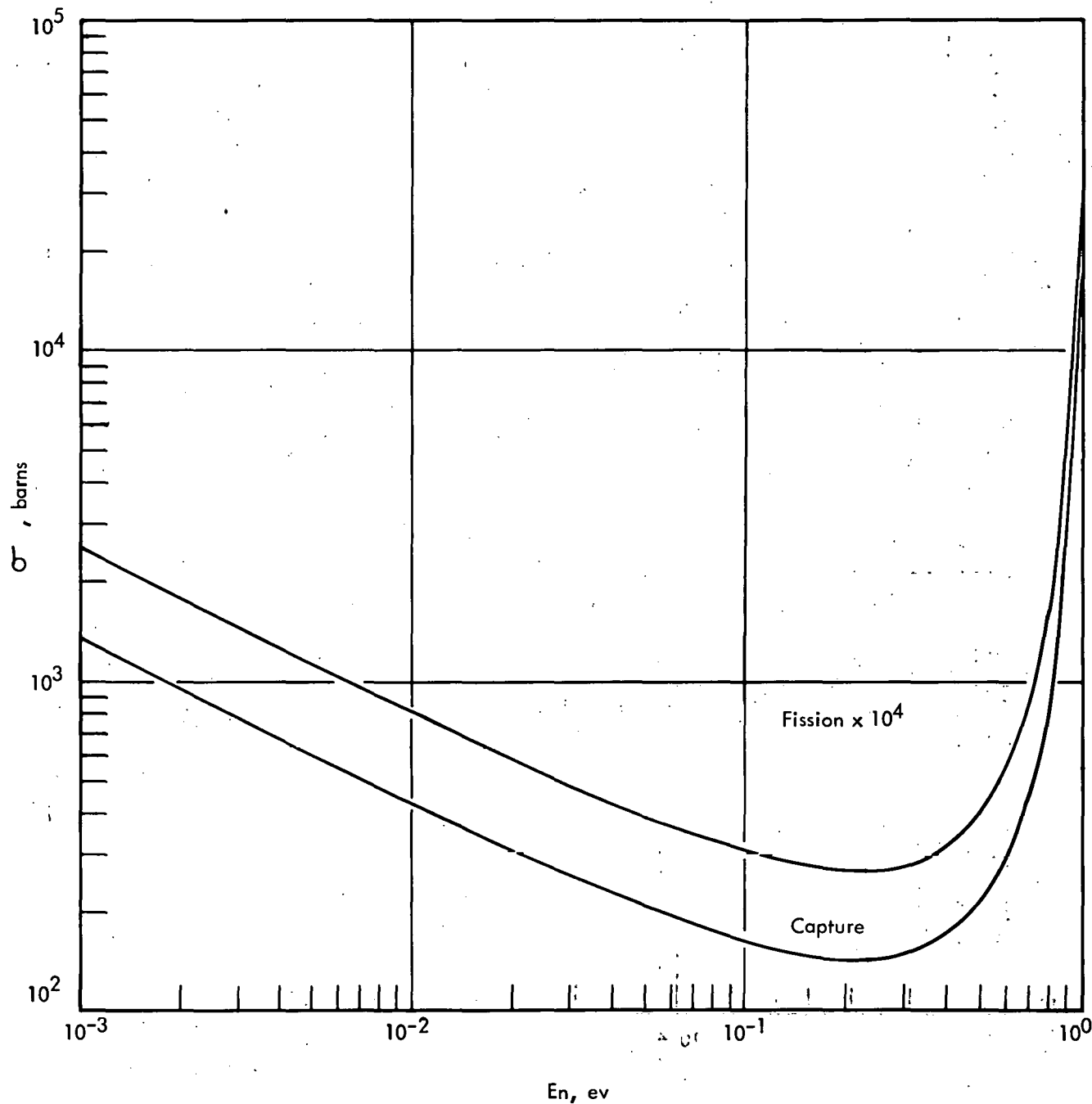
FIG. 2 FISSION AND CAPTURE CROSS SECTIONS, 10^{-3} EV TO 1 EV
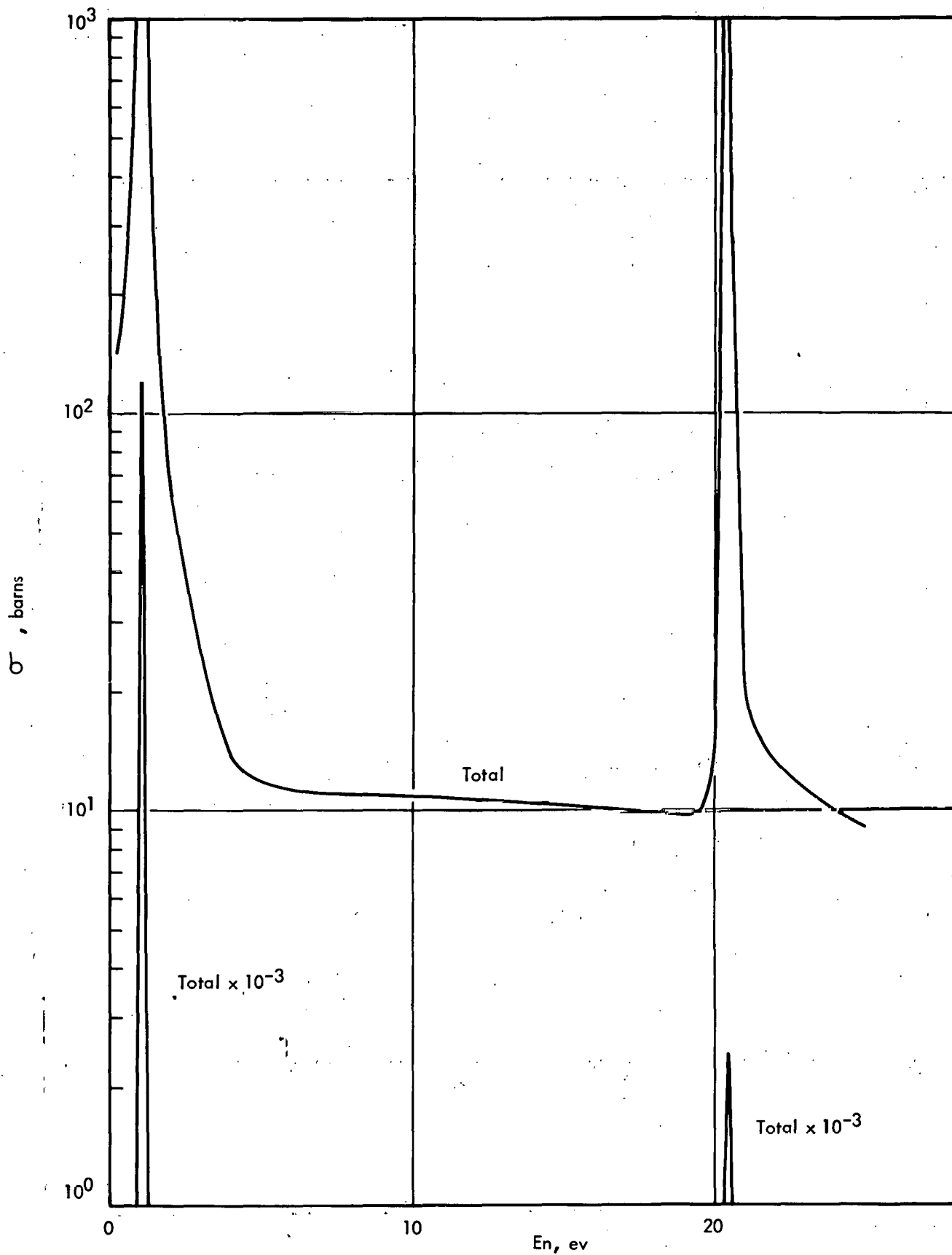
FIG. 3 TOTAL CROSS SECTION, < 25 EV
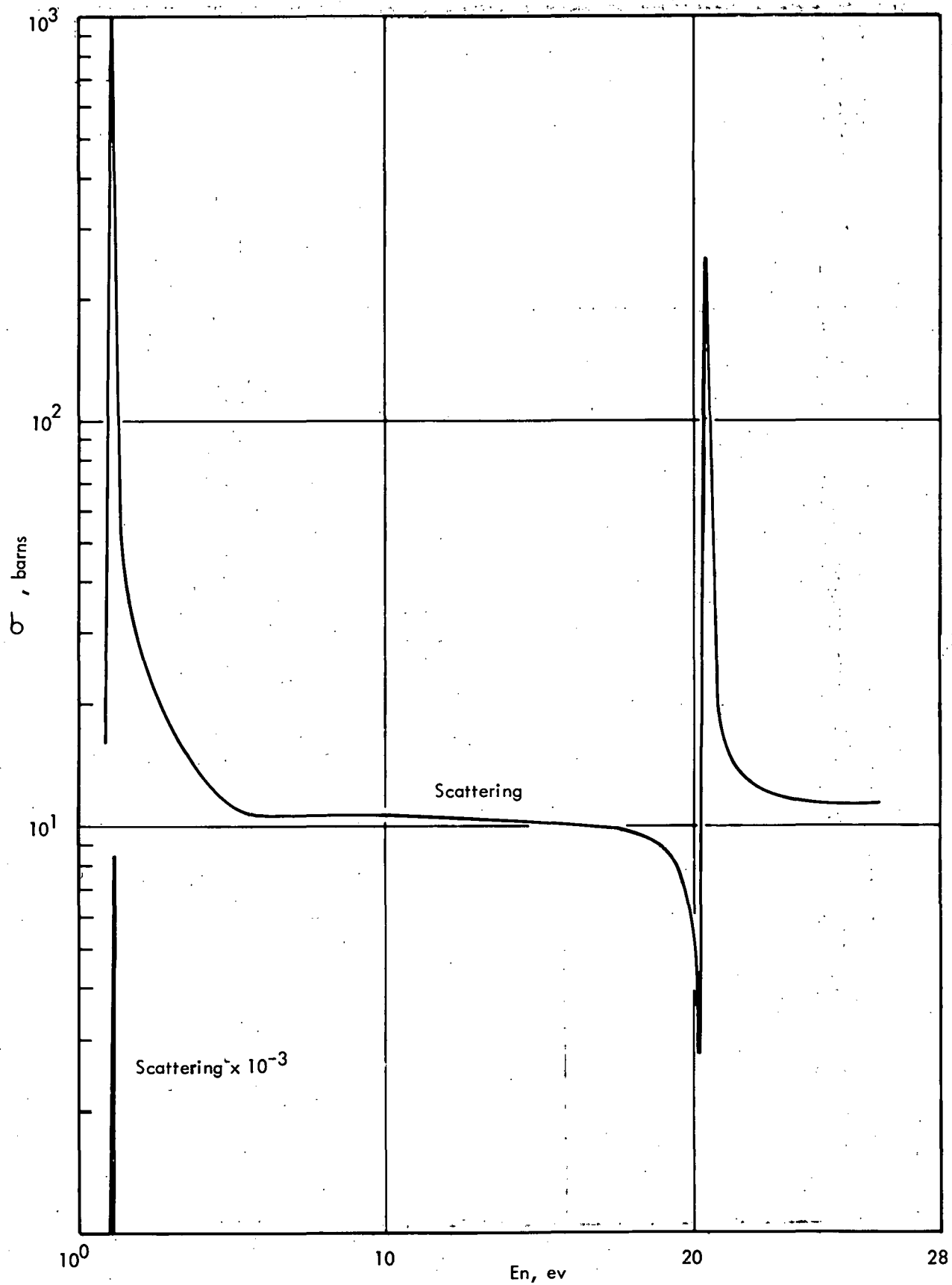
FIG. 4 SCATTERING CROSS SECTION, < 25 EV
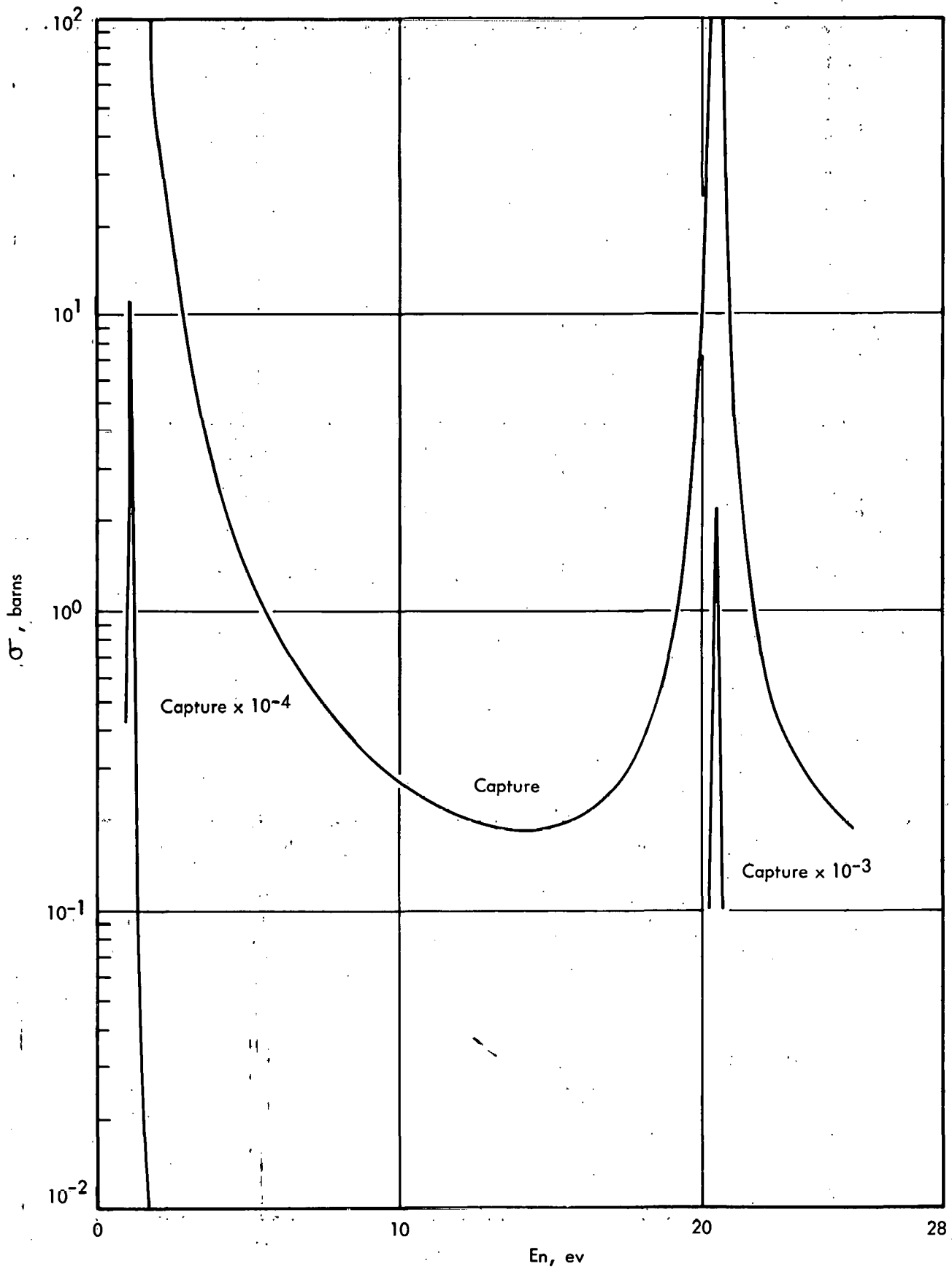
FIG. 5 CAPTURE CROSS SECTION, ⟨25 EV

18
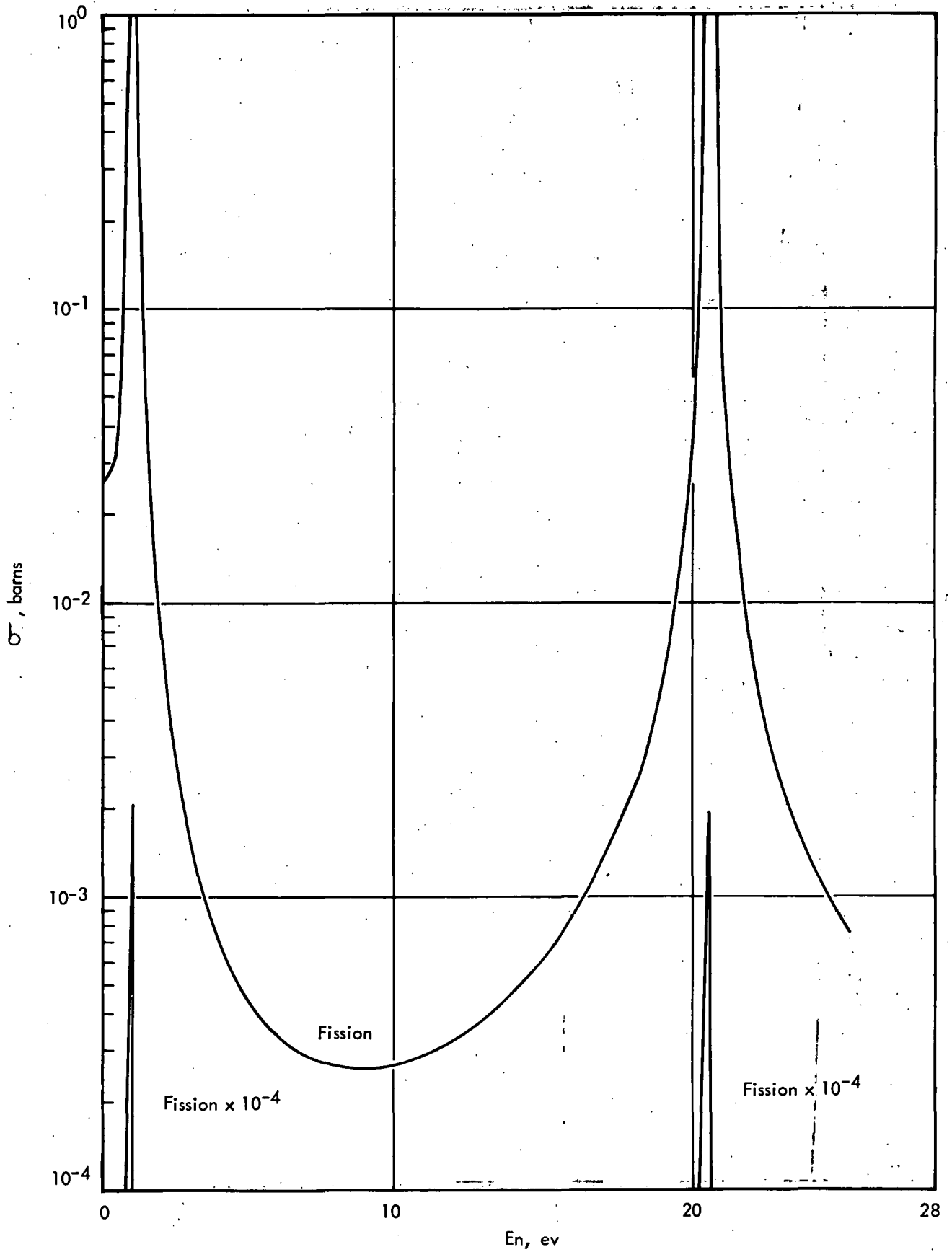
FIG. 6 FISSION CROSS SECTION, ⟨ 25 EV

19
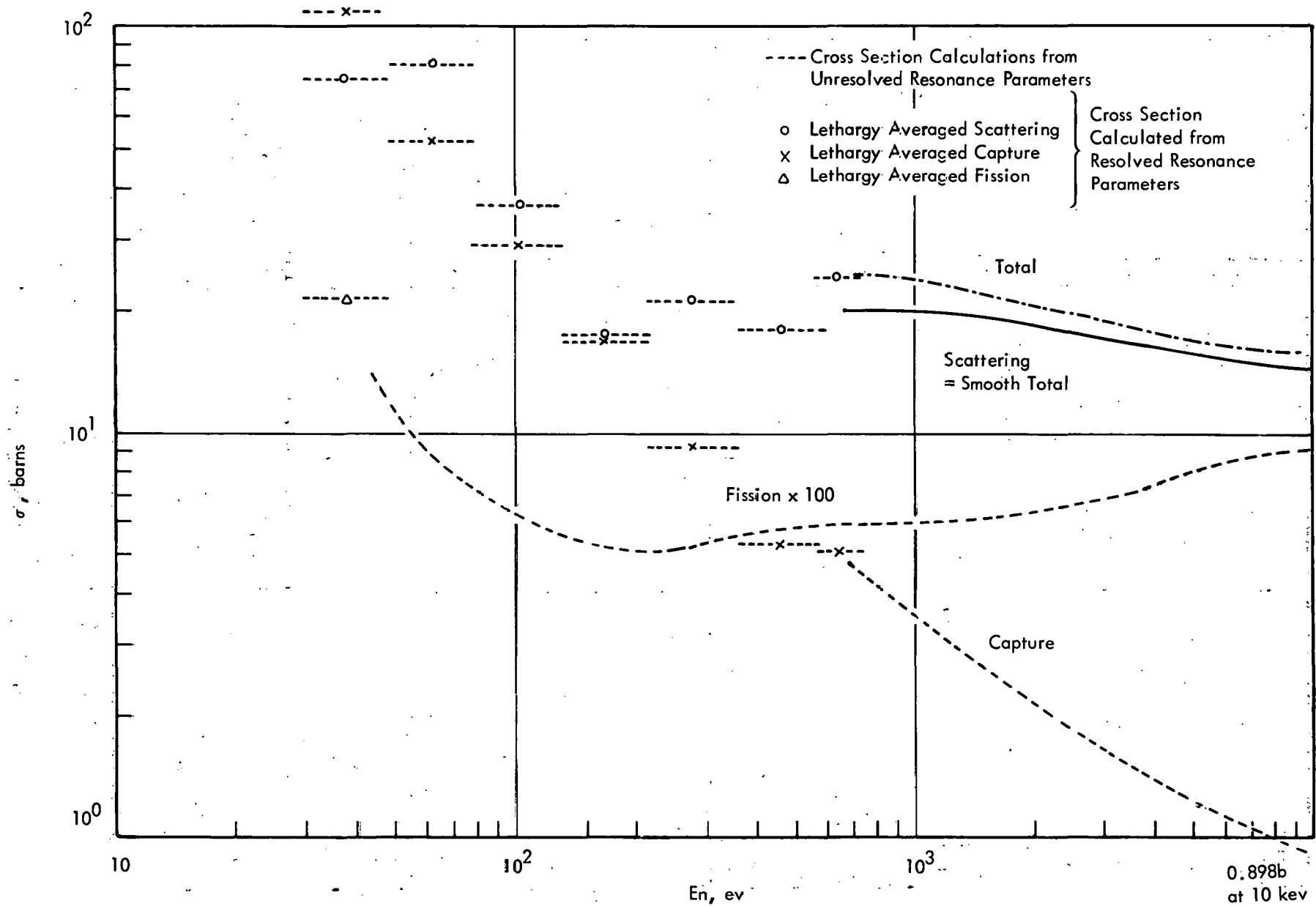
FIG. 7 TOTAL, SCATTERING, FISSION, AND CAPTURE CROSS SECTIONS, ⟨10 KEV

1. Average Level Spacing

Experimental data of Table I up to 680 ev have been used to estimate the average level spacing for the J=1/2 spin state (J=total angular momentum, target spin I=0+). Average values of the experimental data are given in Table II. In addition to the 1 ev resonance, 19 resonances up to 305 ev have been found by Bockhoff and 18 resonances by Asghar and Byers. The 199.6 ev resonance found only by Bockhoff has not been resolved into partial widths, probably indicating a small neutron width and possible p-wave contribution. For 19 resonances up to 305 ev, with the expectation of not more than one missed s-wave resonance, the average level spacing is 16 ev. From 306 to 680 ev, Asghar has found only 16 resonances compared to 22 by Byers and 23 by Bockhoff. The Asghar and Byers data over this energy range are consistent with a level spacing of 16 ev, which was selected for this evaluation.

In this evaluation, the average spacing for the J=3/2 was obtained as 9.65 ev. This value corresponds to the spin dependence of the average spacing based on the Fermi Gas Model

$$D_J \propto \frac{1}{2J+1} \exp\left(\frac{J(J+1)}{2\sigma^2}\right)$$

as obtained by Bethe,[21] or

$$D_J \propto \frac{1}{2J+1} \exp\left(\frac{(J+1/2)^2}{2\sigma^2}\right)$$

as obtained by Newton[22] including shell effects, with $\sigma \approx 3$. (Note: Both of these formulae yield the same ratios for the J=3/2, 1/2 spin states of Pu-240.) The spin cutoff factor σ has an uncertainty ranging from about 2.5 to 5.0. The value of 3 was selected for this evaluation, as a larger p-wave spacing assists in explaining the sharp threshold behavior of the fission cross section (see Sections II-B-4 and III-A).

2. S-Wave Strength Function

The s-wave strength functions obtained from Table I data are given for various energy ranges in Table II. From 0 to 450 ev, values obtained from the data of Bockhoff[5] and Asghar[6] are in good agreement. BNL-325[1] with data only up to 120 ev based largely on the measurements of Simpson,[23] is too small a sample for a reliable estimate of the strength function.

It can be seen from Table II that above 450 ev the strength functions from the Bockhoff and Asghar data are considerably smaller than below 450 ev. The average reduced neutron width of Asghar above 450 ev is 20% larger than the average below 450 ev, as many of the levels with small neutron widths appear to be unresolved. Due to the large number of missed

levels in each set of data above 450 ev, the strength functions are expected to be lower than the 0-450 ev values.

Based on the consistency of the Bockhoff and Asghar data below 450 ev, where nearly all resonances have been resolved by both experimenters, an s-wave strength function of 1.05×10^{-4} ev$^{-1/2}$ is recommended.

3. P-Wave Strength Function

No experimental data on the Pu-240 p-wave strength function have been reported. Various estimates for neighboring nuclei have ranged from 1.25 to 2.5×10^{-4}. Schmidt[24] in a recent evaluation recommends $2.0 \pm 0.3 \times 10^{-4}$ for U-235 and $2.5 \pm 0.5 \times 10^{-4}$ for U-238 and Pu-239. For the ENDF/B evaluation for U-238,[25] a value of 1.58×10^{-4} is recommended based on fitting experimental capture cross sections with unresolved parameters. The present authors also favor a low p-wave strength function for unresolved resonance calculations of U-238 capture to obtain agreement with experimental data. Dunford,[26] based on deformed nucleus optical model calculations, has obtained p-wave strength functions of 1.768 and 1.686 for J=1/2 and J=3/2, respectively, and 1.23 for the s-wave strength function.

In this evaluation, unresolved resonance calculations are used to predict the Pu-240 capture cross section. Based on calculations of U-238 capture and on comparisons of Pu-240 calculated and experimental fission cross sections, a p-wave strength function of 1.75×10^{-4} ev$^{-1/2}$ is favored and used in this analysis.

4. Fission Widths

Fission widths are estimated using the channel theory of fission.[27] To explain the sharp increase in the fission cross section above 200 kev, it is assumed that the fission process in the kev region is dominated by fission through a saddle point state of negative parity which can be reached only by p-wave neutrons.[28,29]

The Hill-Wheeler formula[27] for penetration of the fission barrier gives the relation between the average fission width and the average level spacing as

$$\langle \Gamma_f \rangle_J = \frac{D_J}{2\pi} \sum_i \frac{1}{1 + \exp\left(\frac{2\pi (E_{oi}^J - E)}{E_{b_i}^J}\right)} \quad (1)$$

where $E_{o_i}^J$ is the ith fission barrier position for spin state J, E_{b_i} is the fission barrier width of the ith threshold, and E is the neutron energy (assum-

ing the neutron binding energy corresponds to zero excitation energy for the compound state).

It is assumed that the fission barrier for the $J=1/2^+$ s-wave state is located at energies sufficiently high that the average fission width for this state can be approximated as independent of energy over the energy range of interest. The average fission width for the s-wave state has been estimated as 0.19 mv to obtain approximate agreement with broad energy averages of the preliminary Byers[30] data below 1 kev. Above a few kev, Pu-240 fission is dominated by p-wave fission and only the assumed order of magnitude for the s-wave fission significantly influences the calculated cross section.

It is further assumed that the two p-wave fission thresholds can be approximated by a single barrier position and width. One can then obtain qualitative estimates of the barrier position and width from visual examination of the experimental fission cross section (see Figure 8) which increases from 0.1 barn to 1.5 barns between 0.2 and 1.0 Mev. The barrier position should be located near half the threshold height or about 600 kev and the barrier width should be approximately the width of the threshold based on the slope at the barrier position or about 650 kev. An improved estimate can be obtained by the following procedure. From Equation (1)

$$\ln\left(\frac{1}{W} - 1\right) = \frac{2\pi}{E_b} (E_o - E)$$

$$W = 2\pi\left(\frac{<\Gamma_f>^J}{D^J}\right) \approx \frac{2\pi}{D} \left(\frac{\sigma_f/\sigma_c}{1 - \sigma_f/\sigma_c}\right)\left(\Gamma_n + \Gamma_\gamma + \Gamma_{in}\right)$$

where σ_c is the compound cross section and Γ_{in} is the inelastic scattering neutron width. The approximate form for W is correct only for a single spin state but has been used here with σ_f as the experimental cross section and σ_c as the p-wave compound cross section. From a plot of $\ln$ (1/W-1) versus energy, the barrier position was estimated as 540 kev and the barrier width as 670 kev. Adjustments of these values were then made to improve agreement between calculated and evaluated experimental fission cross sections below 50 kev. The values finally used in this analysis were E_o = 493 kev and E_b = 558 kev.

Since only one fission channel is assumed to be open for each spin state, the fission widths are taken to have a chi-squared distribution with one degree of freedom. The radiation width is taken as constant for all spin states.
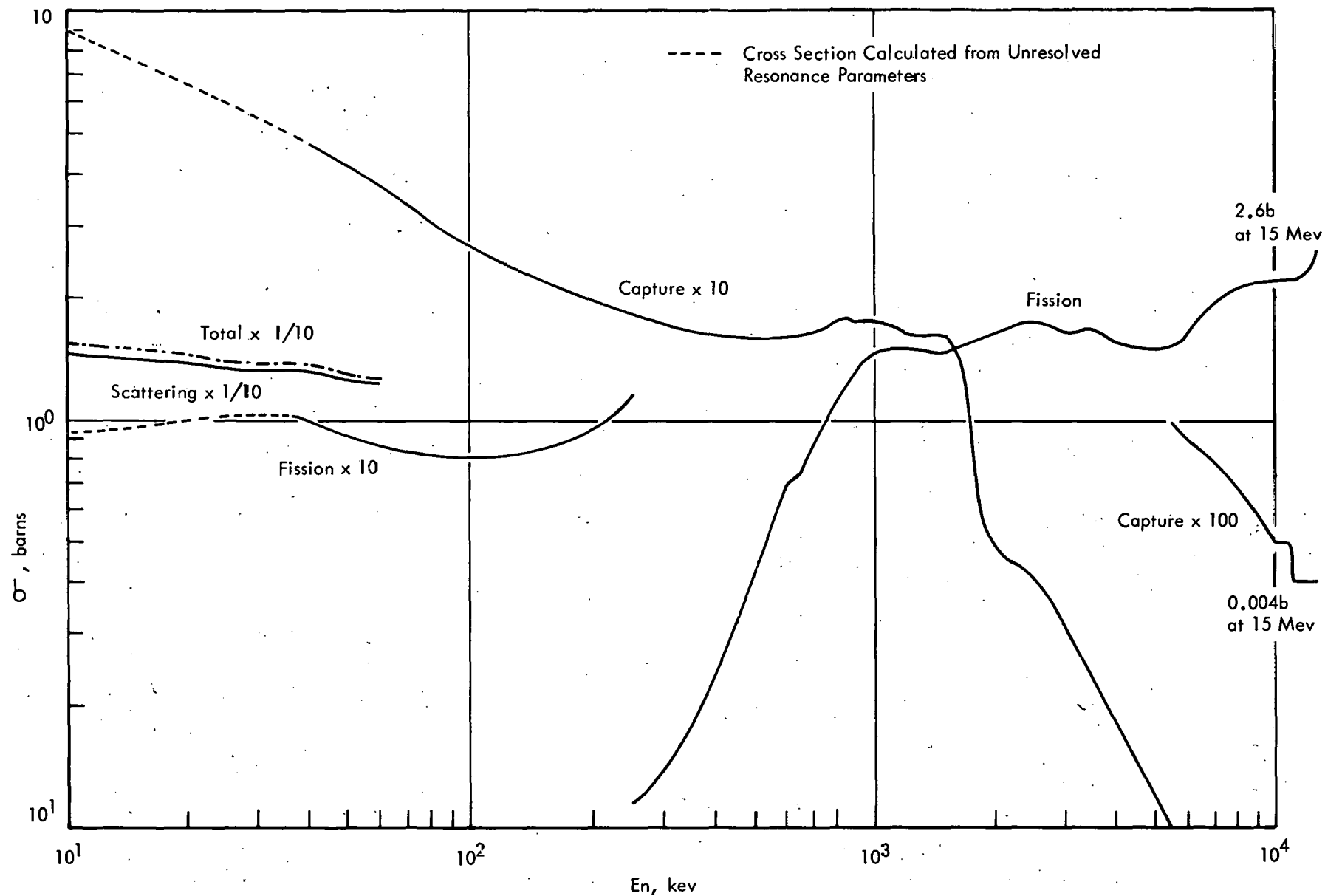
FIG. 8 TOTAL, SCATTERING, FISSION, AND CAPTURE CROSS SECTIONS, > 10 KEV

5. Recommended Parameters

Recommended parameters for the unresolved resonance calculation (0.685 to 40 kev) are given in Table V, where ν_n and ν_n are the chi-squared distribution parameters for scattering and fission. Cross sections calculated from the parameters are given by the dashed curves in Figures 7 and 8. The scattering cross section over this energy range is included in the smooth data file (ENDF/B File 3) and should not be calculated from the parameters.

Near 30 kev, the fission cross section increases slowly with energy as the increase in fission widths with energy is partially compensated by the increase in neutron widths. Above 40 kev, the fission cross section decreases through a minimum near 100 kev due to competition from inelastic scattering. As the fission threshold is approached above 100 kev, the fission widths increase rapidly with energy, causing the sharp increase in the fission cross section.

TABLE V - AVERAGE UNRESOLVED RESONANCE PARAMETERS

Average Reduced Neutron Widths

$\langle \Gamma_n^o \rangle$ $(\ell = 0, J = 1/2) = 1.68 \times 10^{-3}$ ev$^{1/2}$

$\langle \Gamma_n^o \rangle$ $(\ell = 1, J = 1/2) = 2.8 \times 10^{-3}$ ev$^{1/2}$

$\langle \Gamma_n^o \rangle$ $(\ell = 1, J = 3/2) = 1.69 \times 10^{-3}$ ev$^{1/2}$

Average Level Spacing

$\langle D \rangle$ $(J = 1/2) = 16$ ev

$\langle D \rangle$ $(J = 3/2) = 9.65$ ev

Chi-squared Distributions

$\nu_n = 1$ for all spin states

$\nu_f = 1$ for all spin states

Average Radiation Width

$\langle \Gamma_\nu \rangle = 0.03$ ev for all spin states

Average Fission Width, mv

E, ev	$\ell = 0$	$\ell = 1, J = 1/2$	$\ell = 1, J = 3/2$
685	0.19	10	6.03
800	0.19	10	6.03
1000	0.19	10	6.03
2000	0.19	10.2	6.15
4000	0.19	10.39	6.27
6000	0.19	10.62	6.4
8000	0.19	10.93	6.59
10000	0.19	11.00	6.65
15000	0.19	11.58	6.98
20000	0.19	12.04	7.26
25000	0.19	12.89	7.77
30000	0.19	13.21	7.97
35000	0.19	13.79	8.315
40000	0.19	14.47	8.725

THIS PAGE
WAS INTENTIONALLY
LEFT BLANK

III. SMOOTH CROSS SECTIONS

In this chapter, the smooth cross section data are described.

A. FISSION CROSS SECTION

Between a few ev and 10 kev, the only experimental data on the fission cross of Pu-240 at the time of this evaluation are the data of Byers,[7] which are in the form of pointwise cross sections and have considerable structure. In this evaluation, no attempt was made to utilize the detailed Byers data below 10 kev other than to verify the order of magnitude of the cross section. (Note: Since this evaluation was completed, an additional report[31] on this data has been published which includes averages of the fission cross section over energy intervals.)

From 45 ev to 685 ev, the fission cross section is included as smooth data which were calculated using the unresolved parameters discussed in Chapter II. B. Below 300 ev, an s-wave fission width of 0.1 mv, based on an average of the fission widths for the first three resolved resonances, was used for these calculations. The recommended fission width of 0.19 mv was used above 300 ev.

From 685 ev to 40 kev, the fission cross section is to be calculated from the recommended unresolved parameters of Table V. The calculated cross sections using the IDIOT[32] code, which includes the statistical averaging, are shown in Figures 9 and 10. Above 40 kev, the recommended fission cross section is based completely on experimental data, as discussed below.

For this evaluation, experimental data reported as fission ratios of Pu-240/U-235 were normalized to the evaluation of Davey[33] which is based strongly on the U-235 measurements of White[34] while data reported as Pu-240/Pu-239 fission ratios were normalized to the ENDF/B evaluation for Pu-239.[35]

In Figure 9 the experimental fission ratio of Pu-240/U-235 and the recommended fission ratio are shown. In this figure Nesterov's fission ratio of Pu-240/U-235 was derived by combining the measured fission ratio of Pu-240/Pu-239 with the fission ratio of Pu-239/U-235 obtained from Davey's U-235[33] and ENDF/B Pu-239[34] evaluations. In Figure 10 the renormalized experimental fission cross sections and the recommended fission cross section are given. (Note: White and Warner data included in Figure 9 and Figure 10 were not available at the time of this evaluation.)

The energy dependence of the PETREL[30] measurements follows that of other experimental data with notably higher cross sections, considerable structure, and large experimental uncertainties below 200 kev. In this evaluation, the PETREL data were not heavily weighted.

In the energy range from 10 to 100 kev, the recommended cross section was based on Gilboy,[35] Ruddick and White,[36] DeVroey,[37] and Perkin.[38] At 25 kev, the value of Gilboy[35] peaks at this energy, about 20% above the Perkin value. Gilboy notes that his data indicate a possible fission threshold near 10 kev. Based on the agreement of the present calculations with his data, the presence of this low energy threshold is unlikely. The recommended cross section at 25 kev was based on the Perkin data. In this energy range Nesterov's[39] data are about 20% lower than the recommended data, while averages of the Byers[31] data are from 20 to 40% greater than the recommended data.

From 0.1 to 0.3 Mev, the evaluated data was based on the measurements of Ruddick,[36] Gilboy,[35] and Nesterov.[39] The recommended curve is about 15% lower than the two data points of Gilboy near 0.15 Mev and lies within the uncertainties of the data of Ruddick and White. The data of Byers[30] are approximately 20-30% greater than the recommended curve, while Nesterov's data lie 25% below the present data near 0.1 kev with the disagreement decreasing to about 5% near 0.25 Mev.

Between 0.3 and 0.5 Mev, renormalization of the data of Nesterov and Smirenken[40] to the ENDF/B evaluation for Pu-239[40] decreases the authors' values by 10-15%. These data are in agreement with the measurements of DeVroey[37] and Ruddick[36] within the stated uncertainties of the data. Above 0.4 Mev, the data of Byers[7] indicate the same energy dependence of that of Nesterov but are about 20% larger. The recommended curve follows the energy dependence of the Nesterov data in agreement with these data before renormalization and lies within the error bounds of the above mentioned measurements.

Between 0.5 and 4 Mev, the recommended data are based principally on the detailed measurements of Nesterov.[39] Below 0.7 Mev, Byers'[7] data are about 20% above the recommended curve, while above this energy the difference is about 10%. The recommended curve is in agreement with the measurements of Henkel[41] in this energy range.

Above 4 Mev the only detailed measurements are those of Henkel[41] up to 8 Mev, and these data were used in this evaluation. Above 8 Mev, the recommended curve was obtained by extrapolation through the 14 Mev measurements of Nesterov,[42] White,[43] and Kazarinova.[44]

FIG. 9 FISSION RATIOS OF Pu-240/U-235

Legend:
- X NESTEROV [39]
- ⊡ HENKEL [41]
- △ GILBOY [35]
- ▽ RUDDICK [36]
- ◇ WHITE [43]
- Z DEVROY [37]
- ⊀ PERKIN [38]
- ⊕ KAZARINOVA [44]
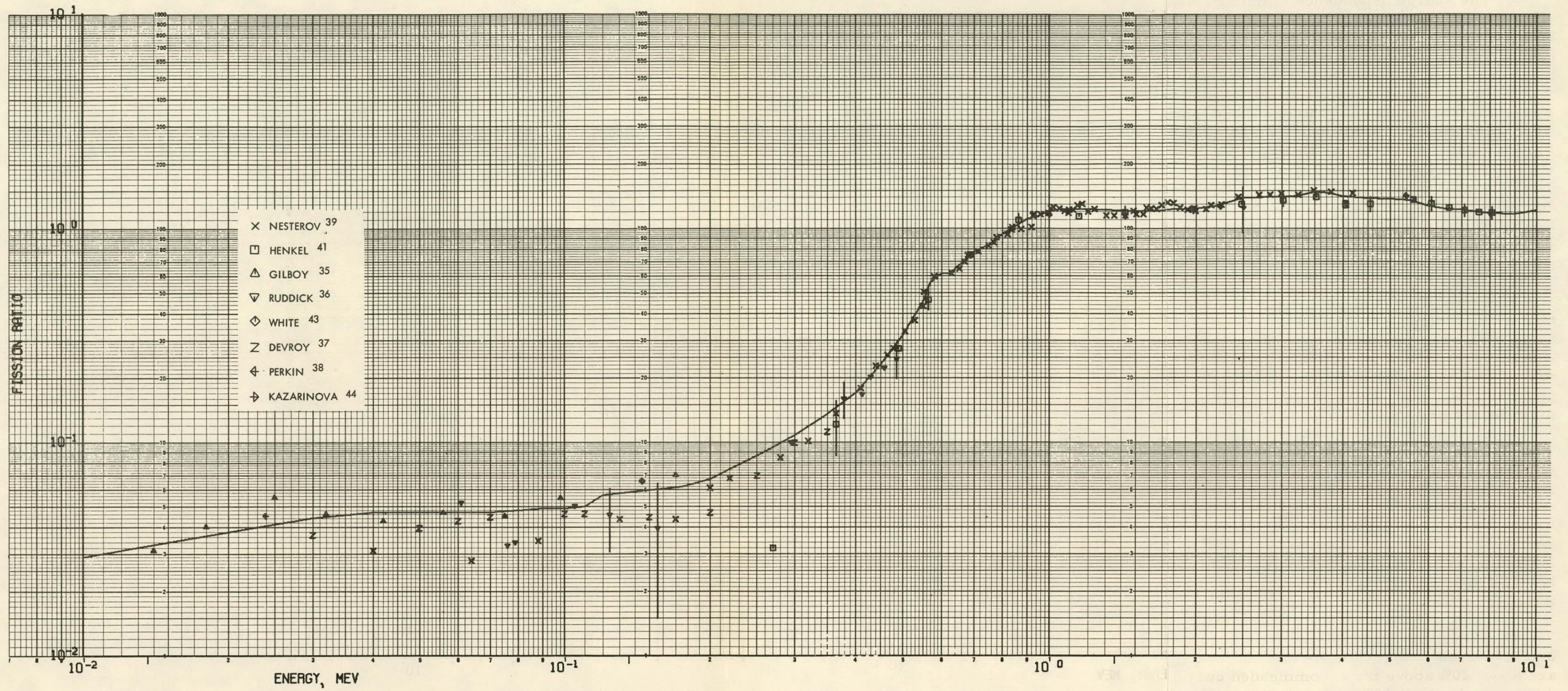
Y-axis: FISSION RATIO
X-axis: ENERGY, MEV
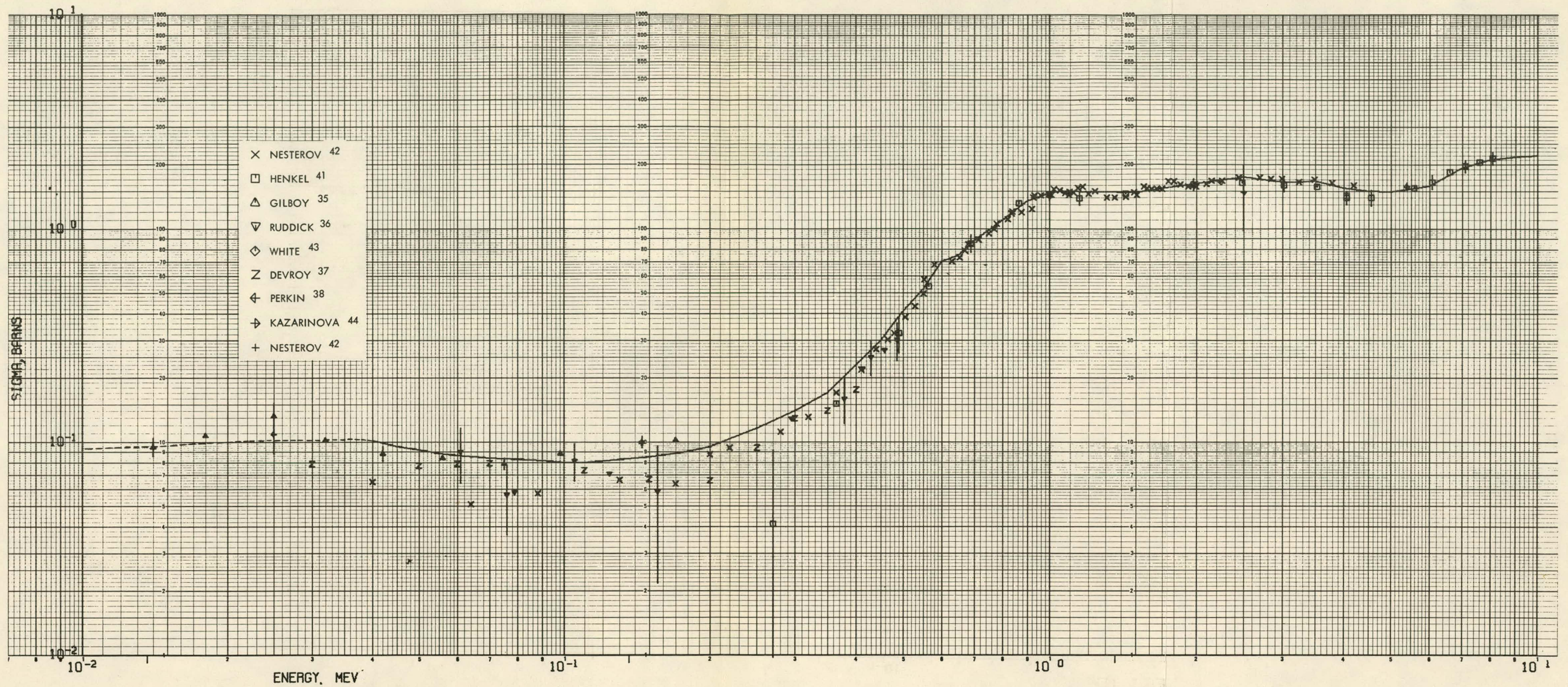
FIG. 10 FISSION CROSS SECTION, > 10 KEV

B. CAPTURE CROSS SECTION

No experimental data on the Pu-240 (n, gamma) cross section above 1 kev have been published. Resonance parameters below 1 kev have been measured and preliminary capture data have been reported by Byers.[7] Douglas[45] reports calculations that indicate the cross section is about 1.75 times the U-238 capture cross section. Details of this calculation are not reported.

In this evaluation, the (n, gamma) cross section has been calculated from the unresolved resonance parameters given in Table V. The calculated cross section below 40 kev is shown in Figures 7 and 8. Above 40 kev, unresolved resonance calculations including averaging over the statistical distributions were made for the Pu-240/U-238 capture ratio. Parameters used for s- and p-waves are those discussed in Chapter II, including the energy-dependent fission widths based on the barrier penetration parameters used below 40 kev. Estimates for the d-wave contribution and competition with inelastic scattering are included in the calculations.

Assuming the d-wave strength function is equal to the p-wave value, the d-wave contribution to the capture cross section was estimated as

$$\frac{\sigma_\gamma(\ell=2)}{\sigma_\gamma(\ell=1)} = \frac{5}{3} \frac{V_{\ell=2} \, \Gamma_{\ell=1}}{V_{\ell=1} \, \Gamma_{\ell=2}} \tag{2}$$

where V_ℓ is the penetration factor for neutrons of the orbital angular momentum ℓ given by Blatt and Weisskopf[46]

$$V(\ell=1) = \frac{R^2/\lambdabar^2}{1 + R^2/\lambdabar^2}$$

$$V(\ell=2) = \frac{R^4/\lambdabar^4}{9 + 3R^2/\lambdabar^2 + R^4/\lambdabar^4}$$

where R is the effective nuclear radius given by 0.87×10^{-12} cm and $\lambdabar$ is the wave length of the neutron. In Equation 2, the 5/3 factor results from the $2\ell+1$ dependence of the compound cross section, and Γ is an average total width for each ℓ state based on neutron widths obtained from a mean level spacing for each state. Calculated U-238 capture cross sections using ENDF/B parameters[25] ($\Gamma_\gamma = .0246$, $D = 18.5$, $S_{\ell=0} = 0.94$) and this d-wave correction agrees with the ENDF/B smooth cross sections up to 600 kev to better than 5%.

The energy dependence of the level density[47] was taken as

$$\langle D \rangle \propto U^2 e^{-2\sqrt{a\,U}}$$

where U is the excitation energy for a neutron binding energy of 5 Mev and a is the level density factor as discussed in Chapter IV.

Inelastic scattering neutron widths were estimated for a 40 kev level by assuming a strength function of 1.75×10^{-4} and including a p-wave penetration factor based on the excess energy above 40 kev. Calculated inelastic scattering cross sections are about 10% below the recommended values near 0.1 Mev, with the discrepancy increasing at higher energies. Calculated fission cross sections agree with the recommended fission cross section within 5% up to 0.2 Mev. Above about 0.3 Mev, the slope of the calculated fission cross section is less than the experimental data with a maximum difference of about 20% up to 500 kev. Calculated fission cross sections are very sensitive to the energy dependence of the level spacing, p-wave strength function, and fission barrier position.

Based on the above comparisons of calculation and experiment, the effects of d-waves, inelastic scattering, and fission on the calculated capture cross section appear to be well approximated up to a few hundred kev. The calculated cross section ratios are given in Table VI. Above 600 kev the ratio approaches 1.1 near 5 Mev.

TABLE VI - CALCULATED Pu-240/U-238 CAPTURE RATIOS

E, kev	Capture Ratio
1	1.27
10	1.2
100	1.24
600	1.2

Some understanding of the uncertainties in this ratio can be seen by noting that the ratio for each spin state is approximately

$$\frac{\sigma_\gamma^{40}}{\sigma_\gamma^{28}} = \frac{\sigma_c^{40}}{\sigma_c^{28}} \frac{\Gamma_\gamma^{40}}{\Gamma_\gamma^{28}} \frac{\Gamma^{28}}{\Gamma^{40}} \propto \frac{S^{40}}{S^{28}} \frac{\Gamma_\gamma^{40}}{\Gamma_\gamma^{28}} \frac{\Gamma^{28}}{\Gamma^{40}}$$

For s-waves above a few kev, $\Gamma \approx \Gamma_n \propto SxD$ and

$$\frac{\sigma_\gamma^{40}}{\sigma_\gamma^{28}} \propto \frac{\Gamma_\gamma^{40}}{\Gamma_\gamma^{28}} \frac{D^{28}}{D^{40}}$$

Until recently the level spacing for Pu-240 was based on data up to 120 ev with level spacing of about 11 ev, which yields upper limits of the capture ratio of about 2 compared to 1.39 for the present data. For small neutron widths $\Gamma \propto \Gamma_\gamma$ and the capture ratio approaches the strength function ratio (about 1.1 for both s and p-waves in this analysis). Near 1 kev the total

width ratio is approximately unity for a cross section ratio of about 1.3 for this evaluation.

The behavior of the ratios shown in Table VI can be qualitatively explained. Above 1 kev to the 10-40 kev range, the small neutron widths for the p-waves leads a p-wave contribution to the capture ratio less than from s-waves. The overall capture ratio then decreases in this energy range. From about 40 kev to near 300 kev, neutron elastic and inelastic widths dominate the total width, leading to an increase in the capture ratio. Below 300 kev fission widths have only a small effect on the p-wave capture cross section. Above 300 kev, the fission widths increase rapidly leading to a decrease in the capture ratio.

C. MEAN NUMBER OF NEUTRONS PER FISSION ($\bar{\nu}$)

The only direct measurements of $\bar{\nu}$ for Pu-240 are those of DeVroey[48] and Kuzminov.[49] Other data based on integral measurements are given in References 50, 51, 52. It is expected that $\bar{\nu}$ for Pu-240 will not differ much from that of Pu-239. The ENDF/B recommended $\bar{\nu}$ for Pu-239,[35] given as a first order polynomial, gives a good fit to the experimental data for Pu-240 below 4 Mev. Above 4 Mev, the only measurement of $\bar{\nu}$ for Pu-240 is that of Kuzminov[49] at 14 Mev. In this evaluation a second order polynomial is recommended. The first two terms are taken to be the same as for Pu-239 in ENDF/B, and a third order term is added to give agreement with the measurement of Kuzminov at 14 Mev. The recommended expression is $\bar{\nu}(E) = 2.87 + 0.135 E (Mev) - 2.04 \times 10^{-3} E^2 (Mev)$. A plot of the recommended $\bar{\nu}$ is given in Figure 11.

D. TOTAL CROSS SECTION

No experimental data are available for the total cross section of Pu-240 above the resolved resonance energy range. As noted by Douglas,[45] the optical model gives justification for choosing the total cross section for Pu-240 to be the same as that for Pu-239. The recommended total cross section of Douglas, which is based on experimental measurements for Pu-239, was selected for this evaluation above 1 kev. For the resolved resonance region up to 685 ev, the total cross section is to be calculated from the resonance parameters of Table III. Graphs of the total cross section are given in Figures 1, 3, 7, 8, and 12.

E. NONELASTIC CROSS SECTION

From optical model considerations, nonelastic cross sections do not change significantly with small changes in atomic mass when the energy of the incident neutrons is sufficiently high.[45] Optical model calculations yield the total cross section σ_t, the shape elastic cross section σ_{se}, and the absorption cross section σ_a
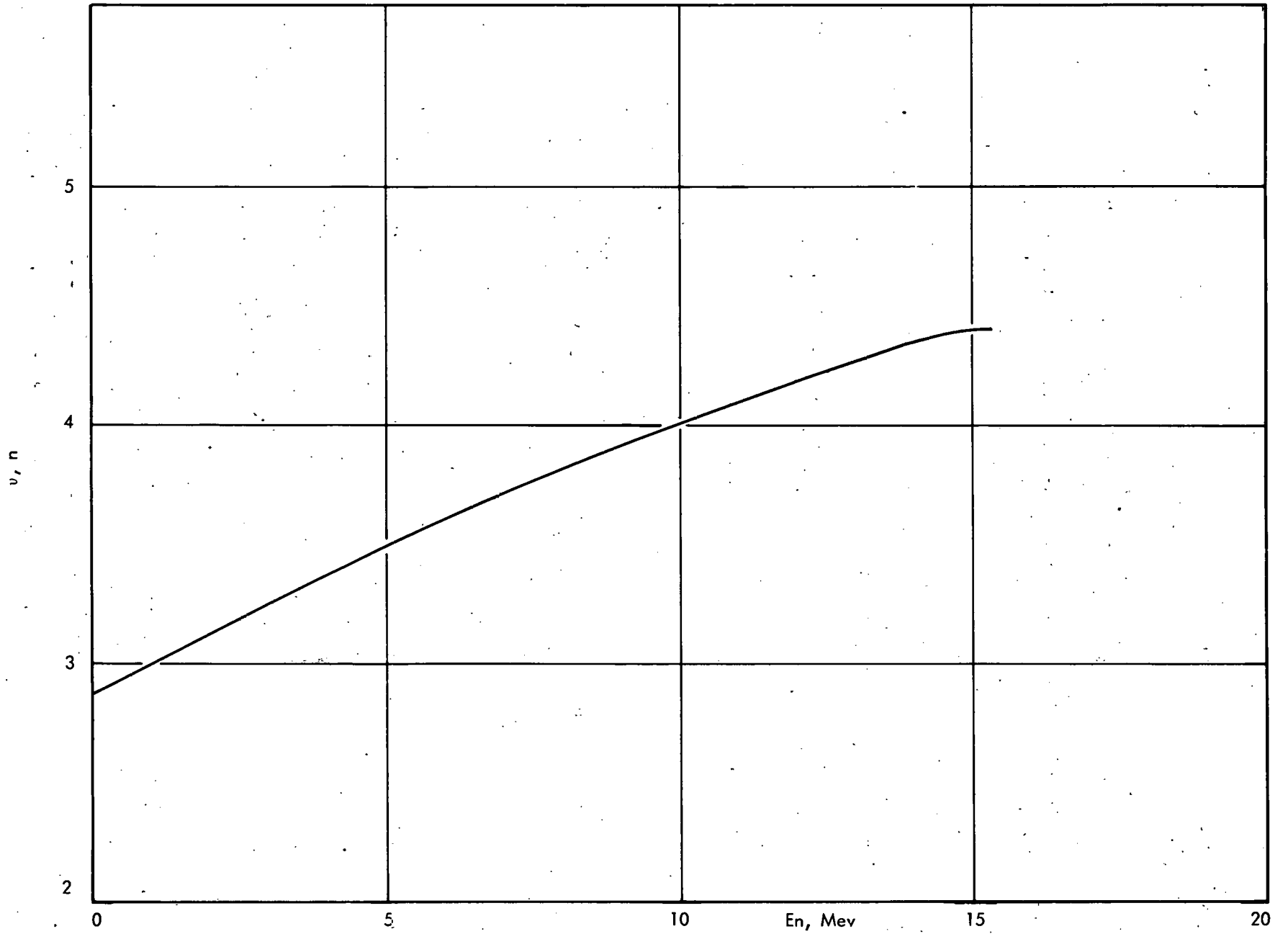
FIG. 11 MEAN NUMBER OF NEUTRONS PER FISSION, $\overline{\nu}$

34
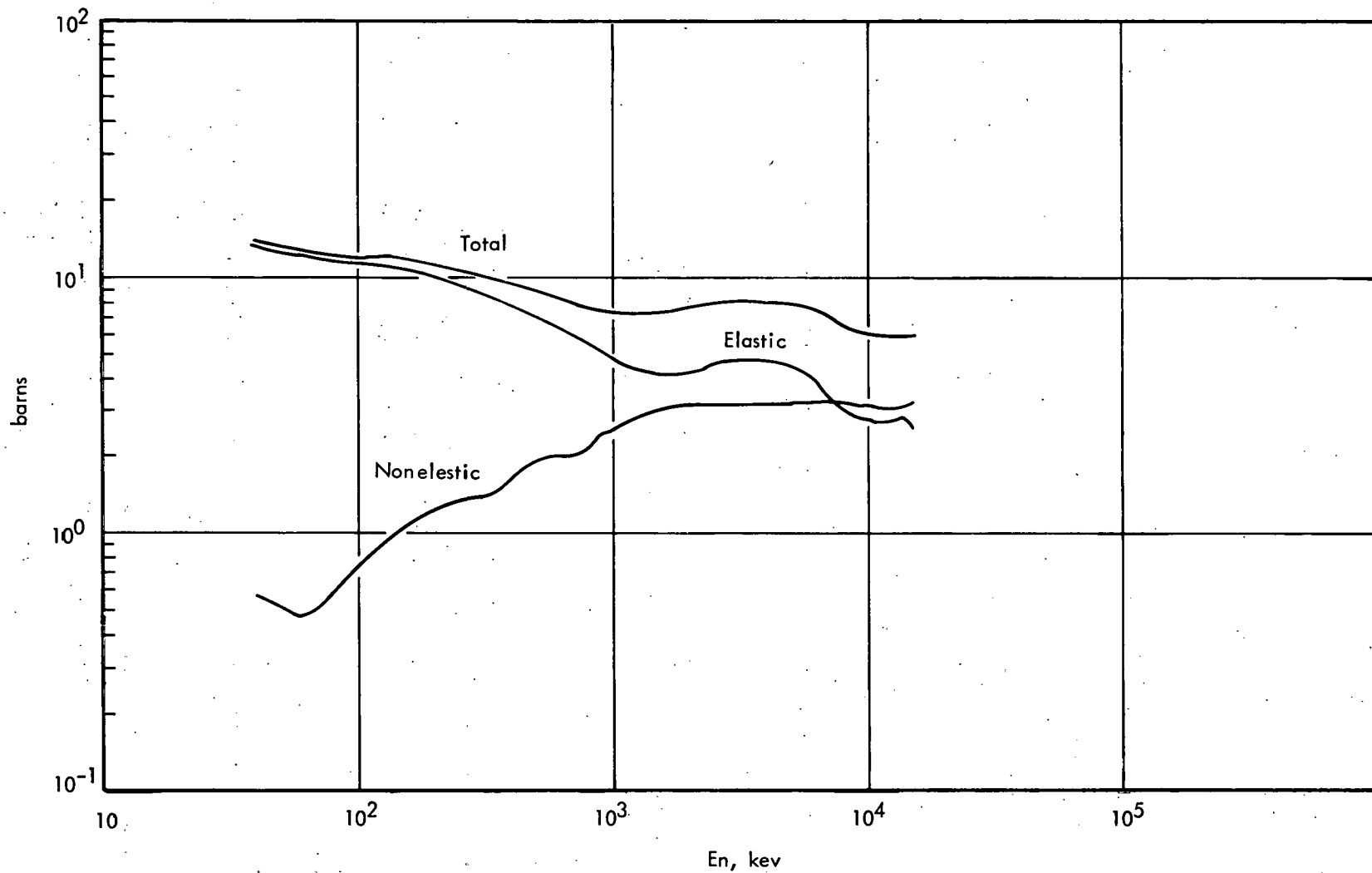
FIG. 12 TOTAL, ELASTIC SCATTERING, AND NONELASTIC CROSS SECTIONS, >40 KEV

where

$$\sigma_t = \sigma_{se} + \sigma_a$$

$$\sigma_a = \sigma_{ce} + \sigma_{ne}$$

$$\sigma_n = \sigma_{se} + \sigma_{ce}$$

In these equations, σ_{ce} is the compound elastic scattering, σ_n is the experimentally observed elastic scattering, and σ_{ne} is the nonelastic cross section.

At high energies, approximately 2 Mev for heavy nuclei such as Pu, σ_{ce} is small because of the large number of channels available for compound nucleus decay. Then based on the assumption that σ_a varies only slightly with mass, the nonelastic cross section for Pu-240 above 2.5 Mev was taken to be the same as for Pu-239 in the ENDF/B evaluation.[10] Below 2.5 Mev, the Pu-240 nonelastic cross section was taken to be the same as for the ENDF/B evaluation of U-238[25] based on the similarity of nuclear properties for these two nuclei. Below 40 kev, the nonelastic cross section is to be calculated from the resolved and unresolved resonance parameters. The nonelastic cross section above 40 kev is shown in Figure 12.

F. ELASTIC SCATTERING

The elastic scattering cross section was obtained by subtraction of the nonelastic cross section from the total cross section. Below 685 ev, the scattering cross section is to be calculated from the resolved resonance parameters. Graphs of the cross section are given in Figures 1, 4, 9, 10, and 12.

G. ANGULAR DISTRIBUTIONS FOR ELASTIC SCATTERING

Evaluated data for the average cosine of the scattering angle $\bar{\mu}$, the average logarithmic energy loss ζ, the Grueling-Goertzel parameter γ, and Legendre polynomial expansions of the scattering angle were obtained from H. Alter.[53] A plot of $\bar{\mu}$ is given in Figures 13 and 14.

H. (n, 2n) AND (n, 3n) REACTIONS

The recommended cross sections for (n, 2n) and (n, 3n) reactions were obtained from calculations of Pearlstein[53] and are graphed in Figure 15.

I. INELASTIC SCATTERING

The total inelastic scattering cross section was obtained by subtracting the evaluated fission, capture, (n, 2n), and (n, 3n) cross sections from the nonelastic cross section and is shown in Figures 16 and 17.
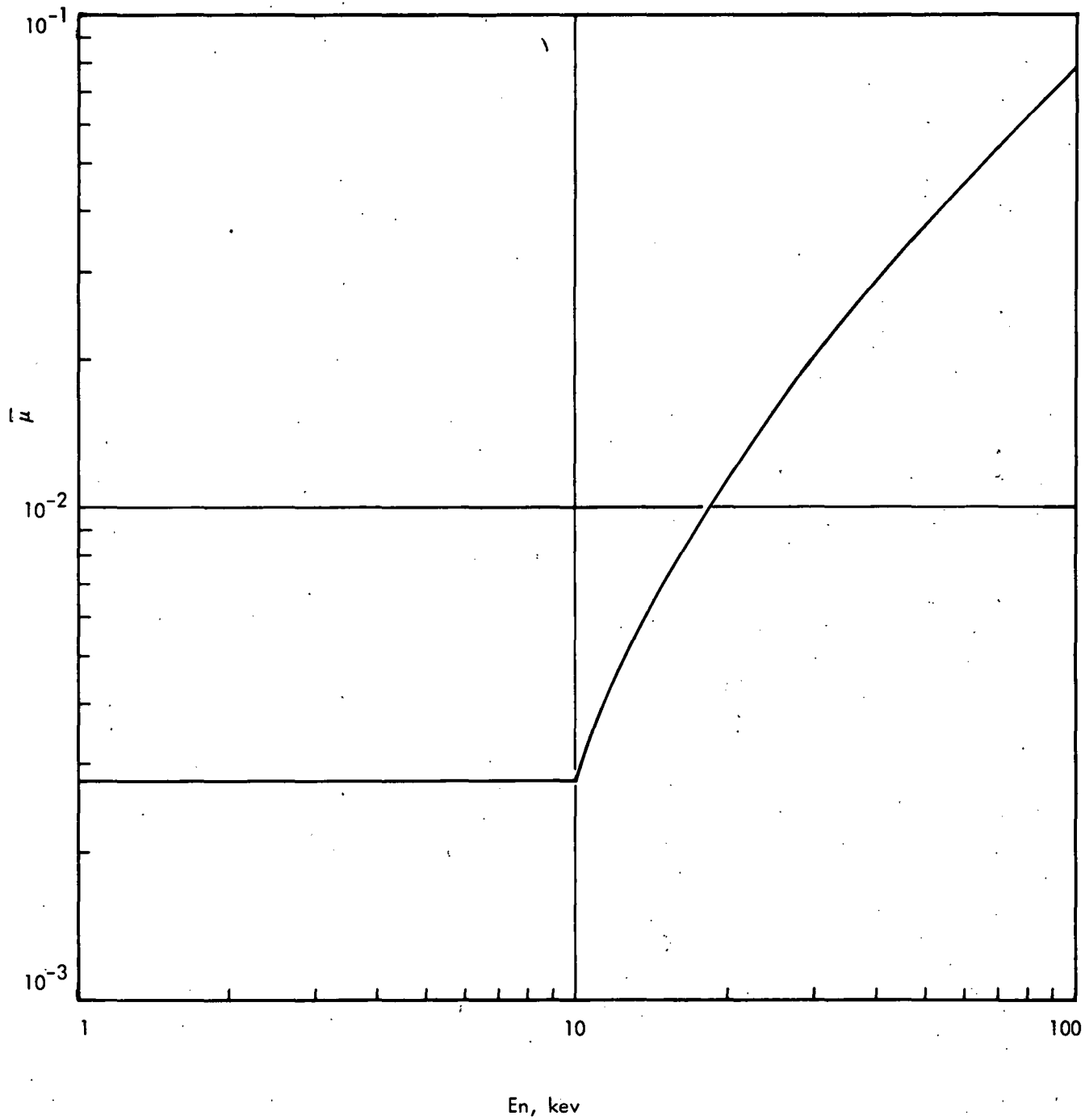
FIG. 13 AVERAGE COSINE OF SCATTERING ANGLE, $\bar{\mu}$
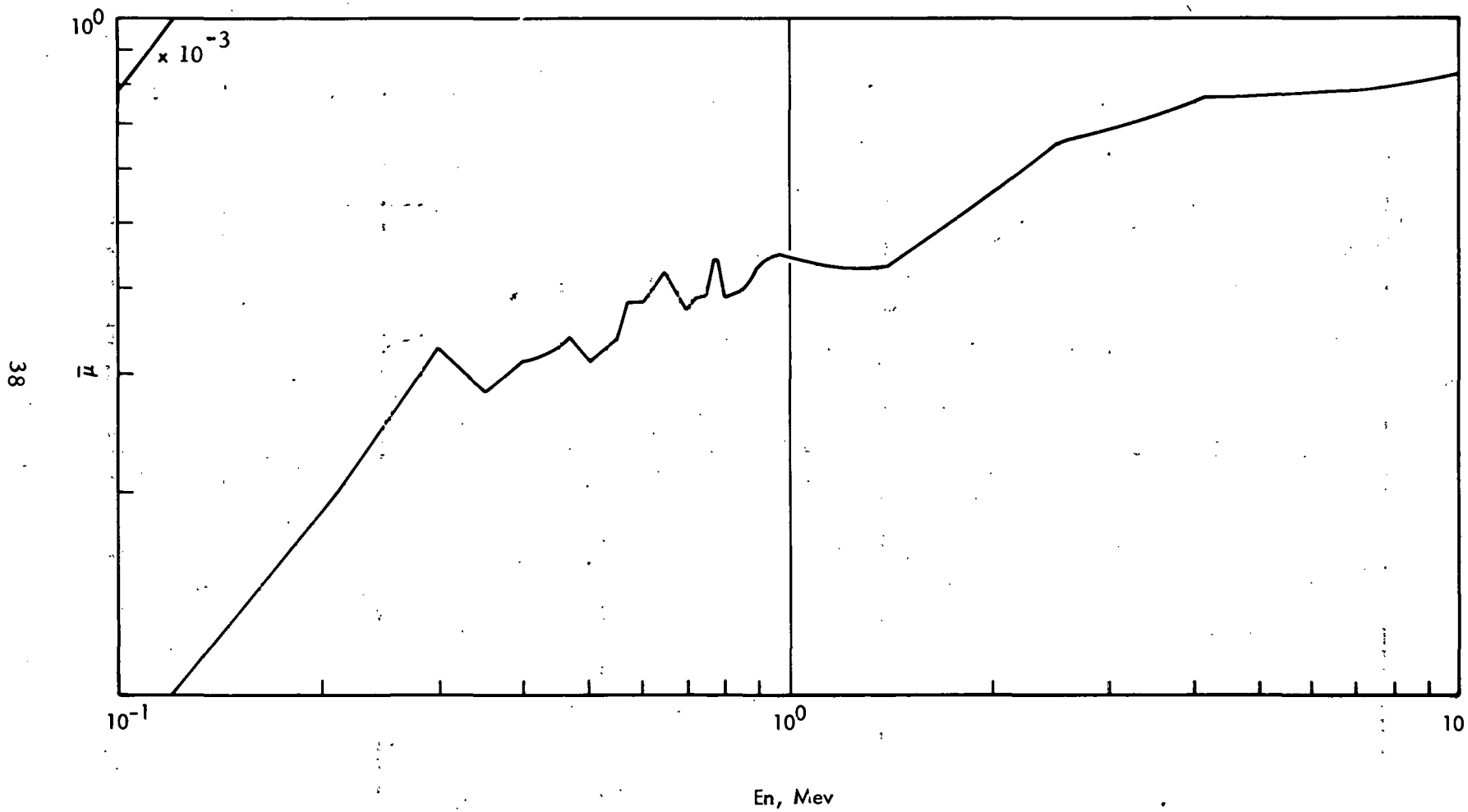
FIG. 14 AVERAGE COSINE OF SCATTERING ANGLE, $\bar{\mu}$

38
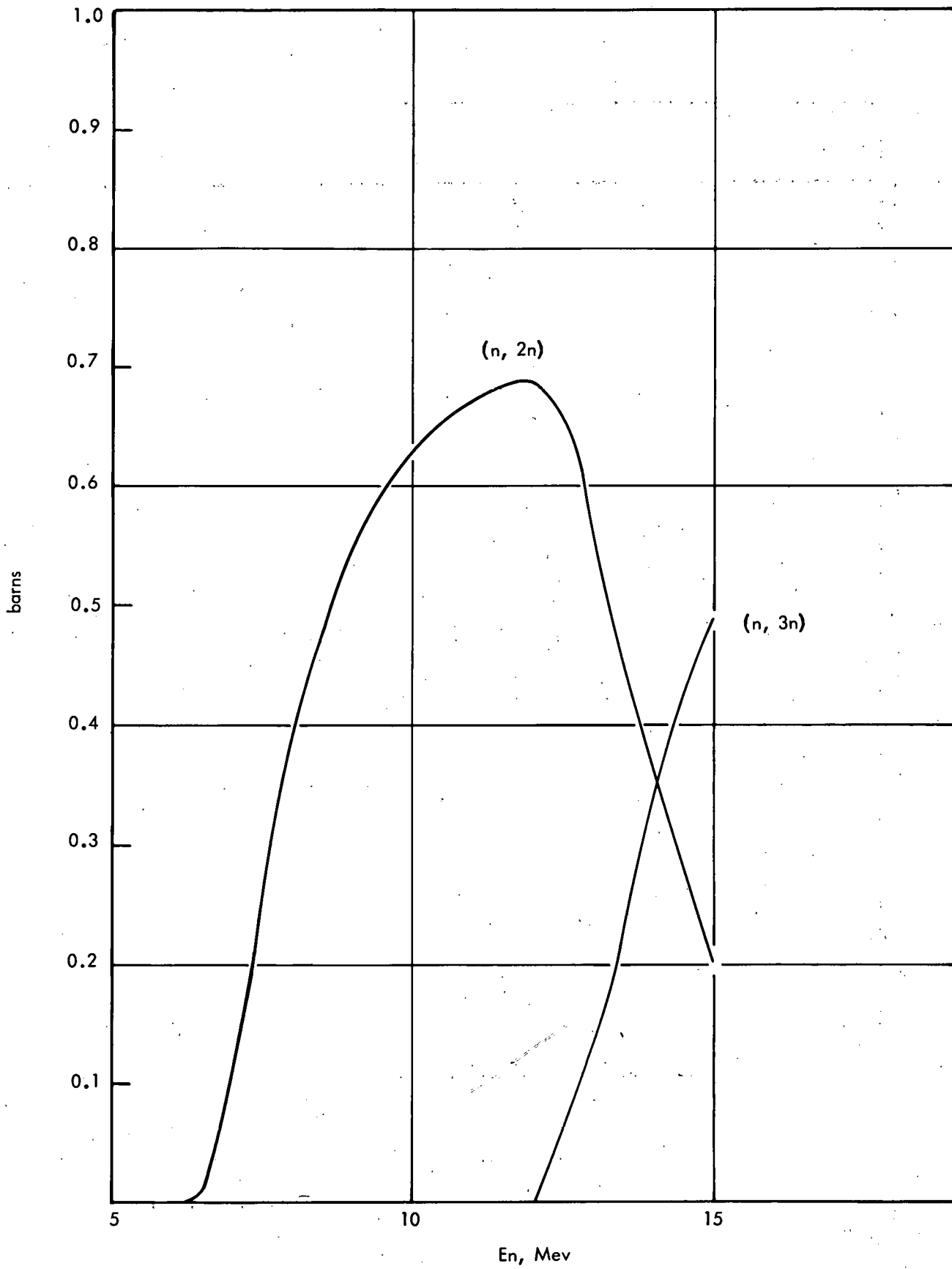
FIG. 15 (N, 2N) AND (N, 3N) CROSS SECTIONS
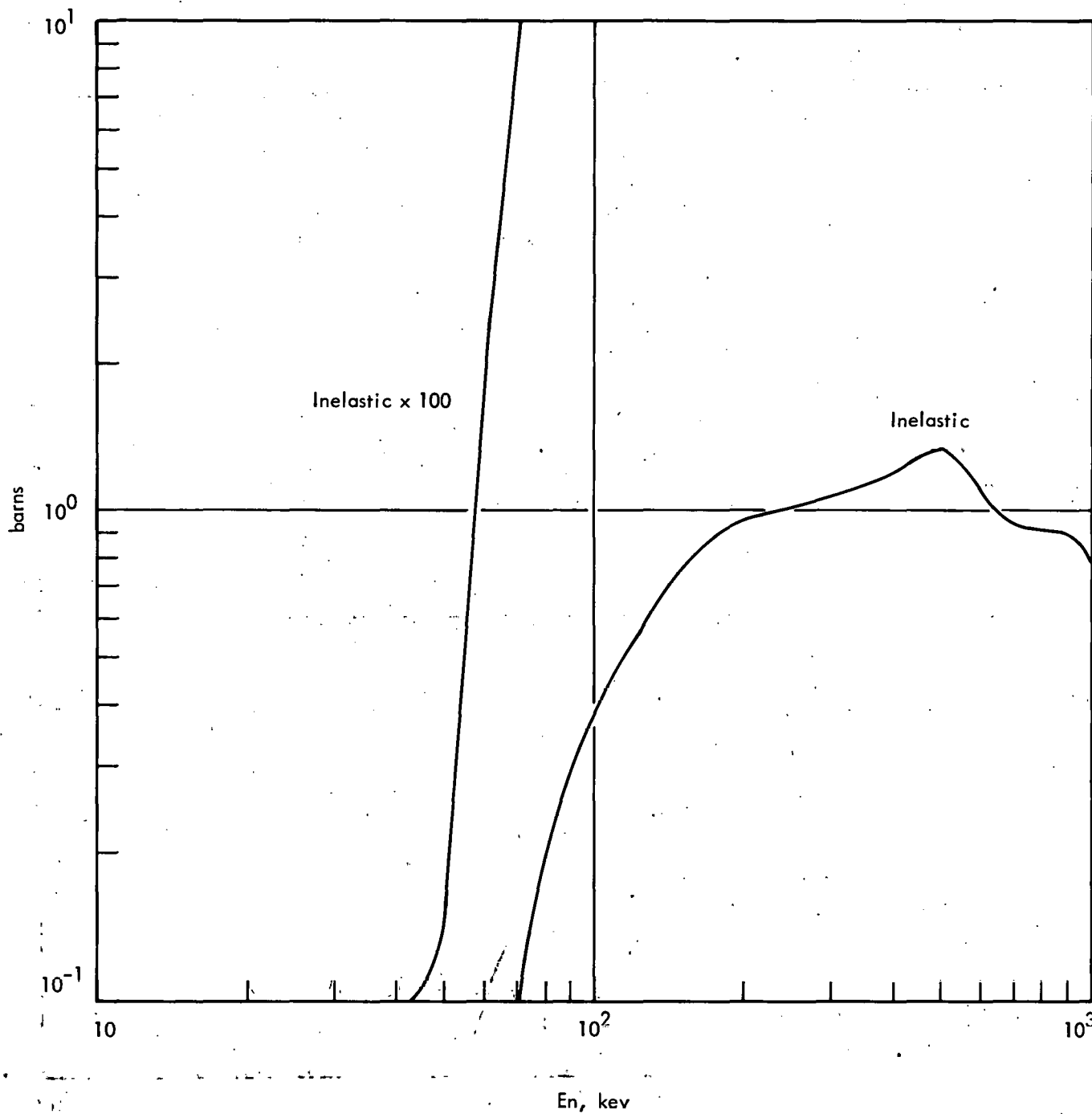
FIG. 16 TOTAL INELASTIC CROSS SECTIONS

40
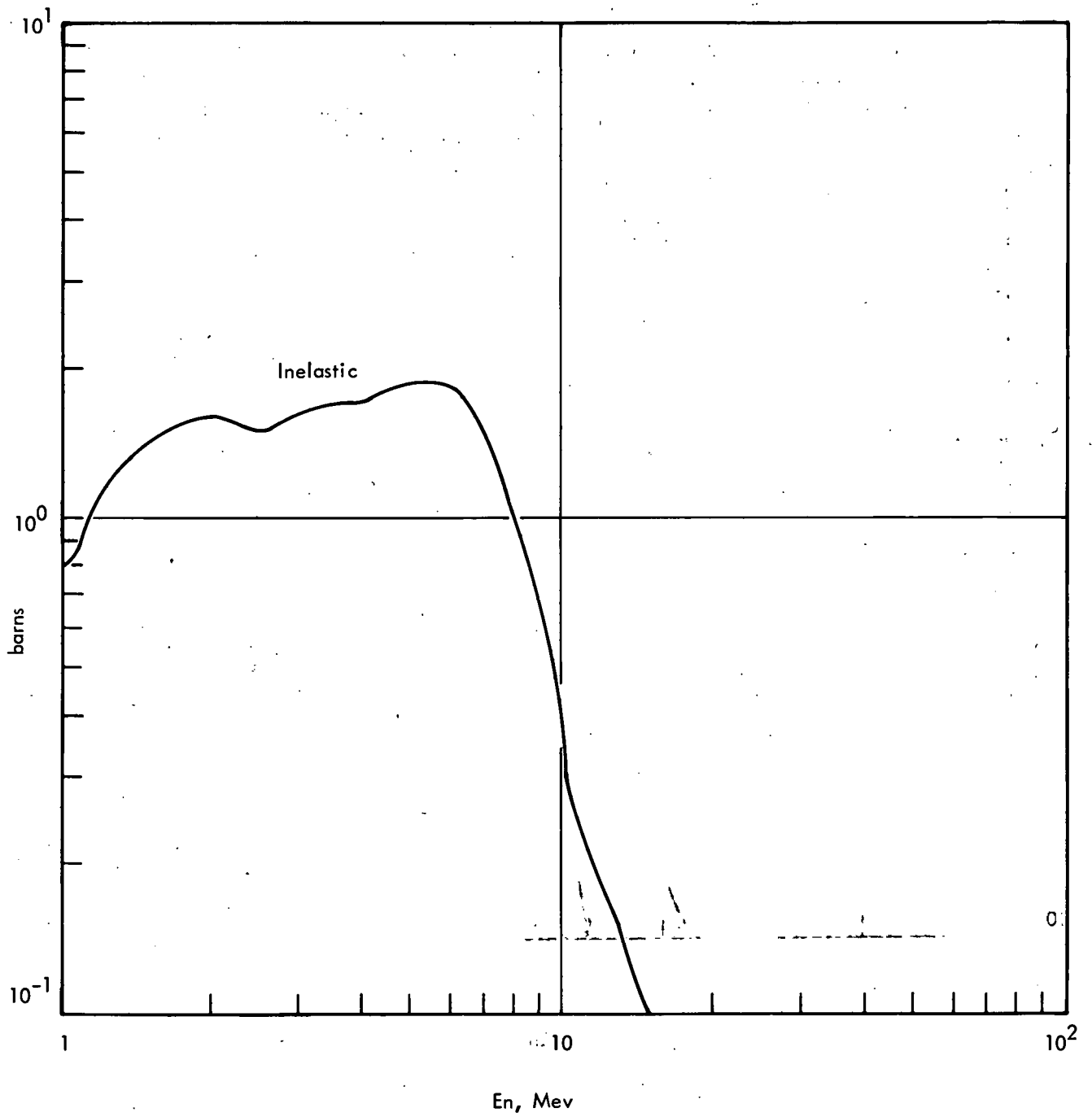
FIG. 17 TOTAL INELASTIC CROSS SECTIONS

Inelastic scattering is treated as completely resolved into six levels up to 2 Mev with a statistical distribution assumed above this energy. Separation of the total inelastic cross section into six levels at 0.043, 0.142, 0.292, 0.600, 1.0, and 1.55 Mev follows that used by Douglas[45] and Drake.[56] Below 600 kev and above 1 Mev, the proportions of the first three levels are assumed to be the same as for U-238. The inelastic scattering cross section for U-238 in ENDF/B[25] was used for this purpose. Because of the sharply increasing fission competition between 0.6 and 1 Mev, significant differences between Pu-240 and U-238 are expected. In these energy ranges, a smooth extrapolation was made for each of the three levels between their values at 0.6 and 1.0 Mev. For the three levels between 0.6 and 1.55 Mev, the relative proportions of these levels were assumed to be the same as used by Drake.[56]

Cross sections for each of the resolved levels are given in Figures 18 and 19.
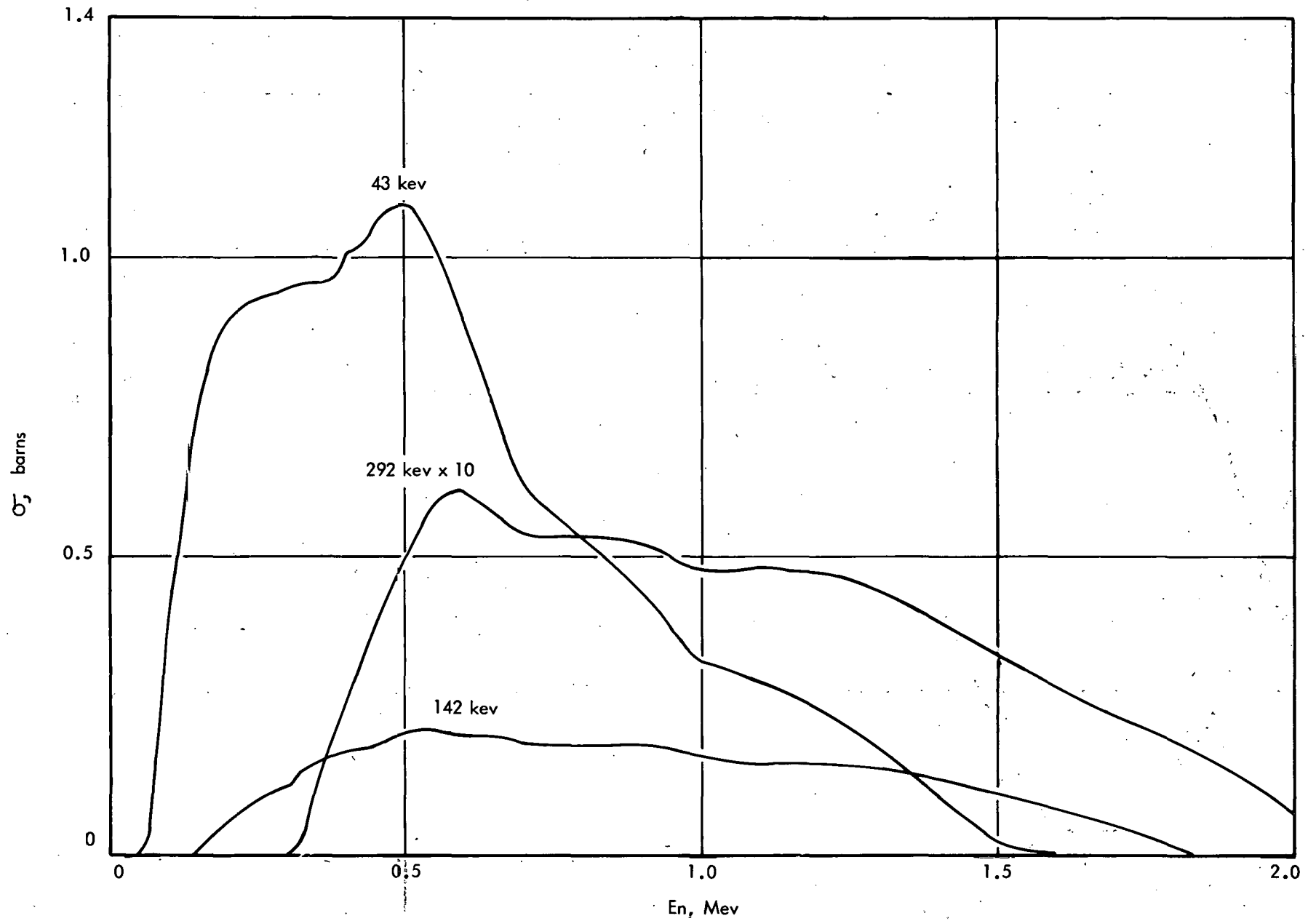
FIG. 18 PARTIAL INELASTIC CROSS SECTIONS

43
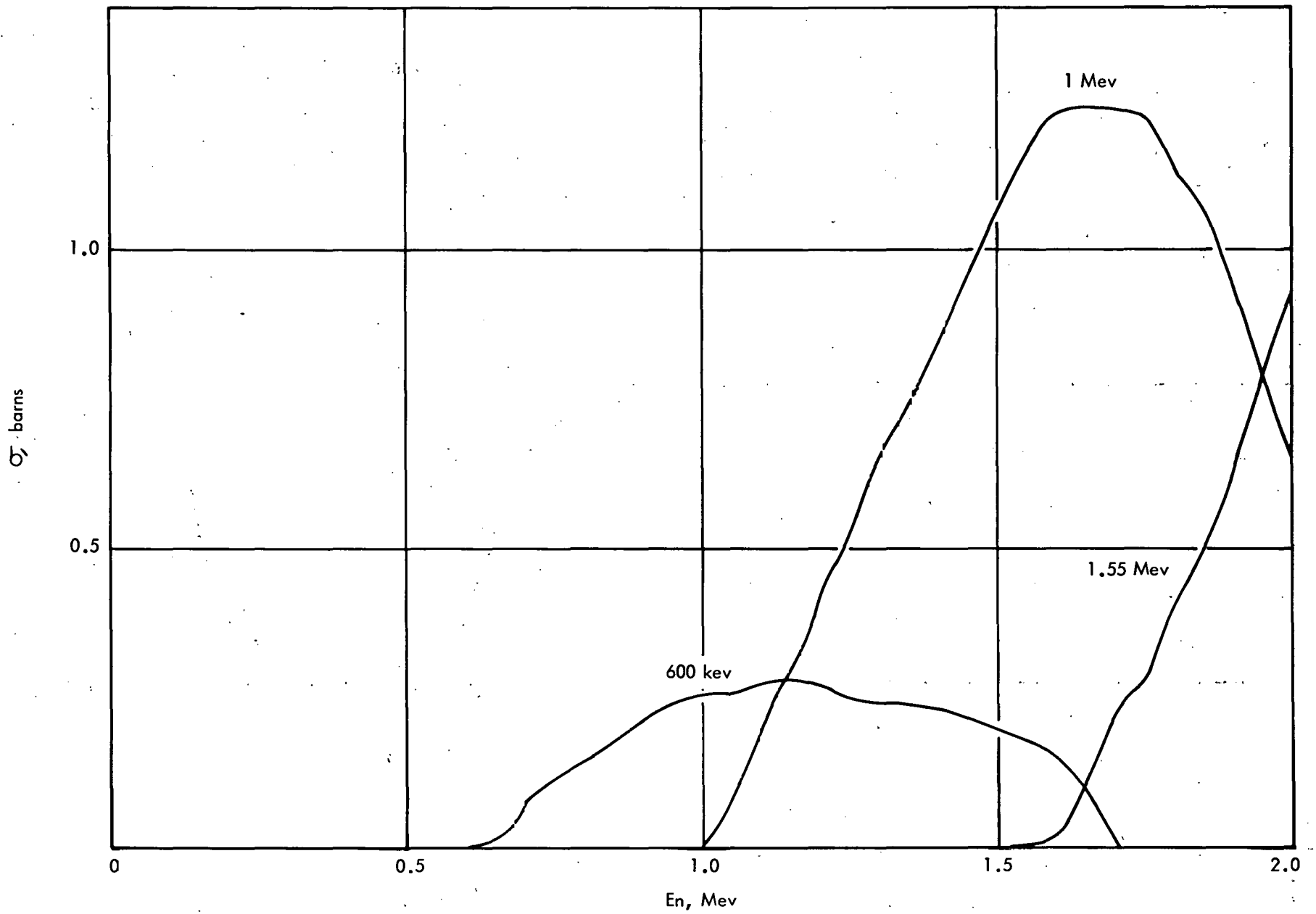
FIG. 19 PARTIAL INELASTIC CROSS SECTIONS

IV. SECONDARY ENERGY DISTRIBUTIONS

A. INELASTIC SCATTERING

The secondary energy distribution for each of the six resolved levels given in Chapter III.I is taken as a discrete energy loss (LF=3 in ENDF/B formats) with the energy loss corresponding to the energy of the level.

Above 2 Mev, a statistical distribution is assumed with the energy loss described by a Maxwellian distribution with energy-dependent nuclear temperature (LF=9). Nuclear temperatures were estimated as

$$\theta = \left(\frac{E}{a}\right)^{1/2}$$

$$a^{1/2} = \frac{A^{1/2}}{3.18}$$

where a is the level density parameter, E is the incident neutron energy, and A is the atomic mass. The constant 3.18 was obtained by fitting this expression to experimental data of the nuclear temperature for inelastic scattering of U-238. Figure 20 shows the recommended temperature.

B. FISSION NEUTRON DISTRIBUTION

For the secondary energy of fission neutrons, a Maxwellian distribution (LF=8) is assumed with the maxwellian temperature obtained from Terrell's formula[54] for the average energy of the prompt fission neutrons given by

$$\overline{E} = 0.75 + 0.65 \sqrt{\overline{\nu}+1}$$

The relation between the Maxwellian temperature and the average neutron energy is

$$\theta = \overline{E}/2$$

For $\overline{\nu}$ in this expression an average of the recommended $\overline{\nu}$ (E) from 0.3 to 2 Mev was used. The recommended temperature for the fission distribution is 1.37 Mev.
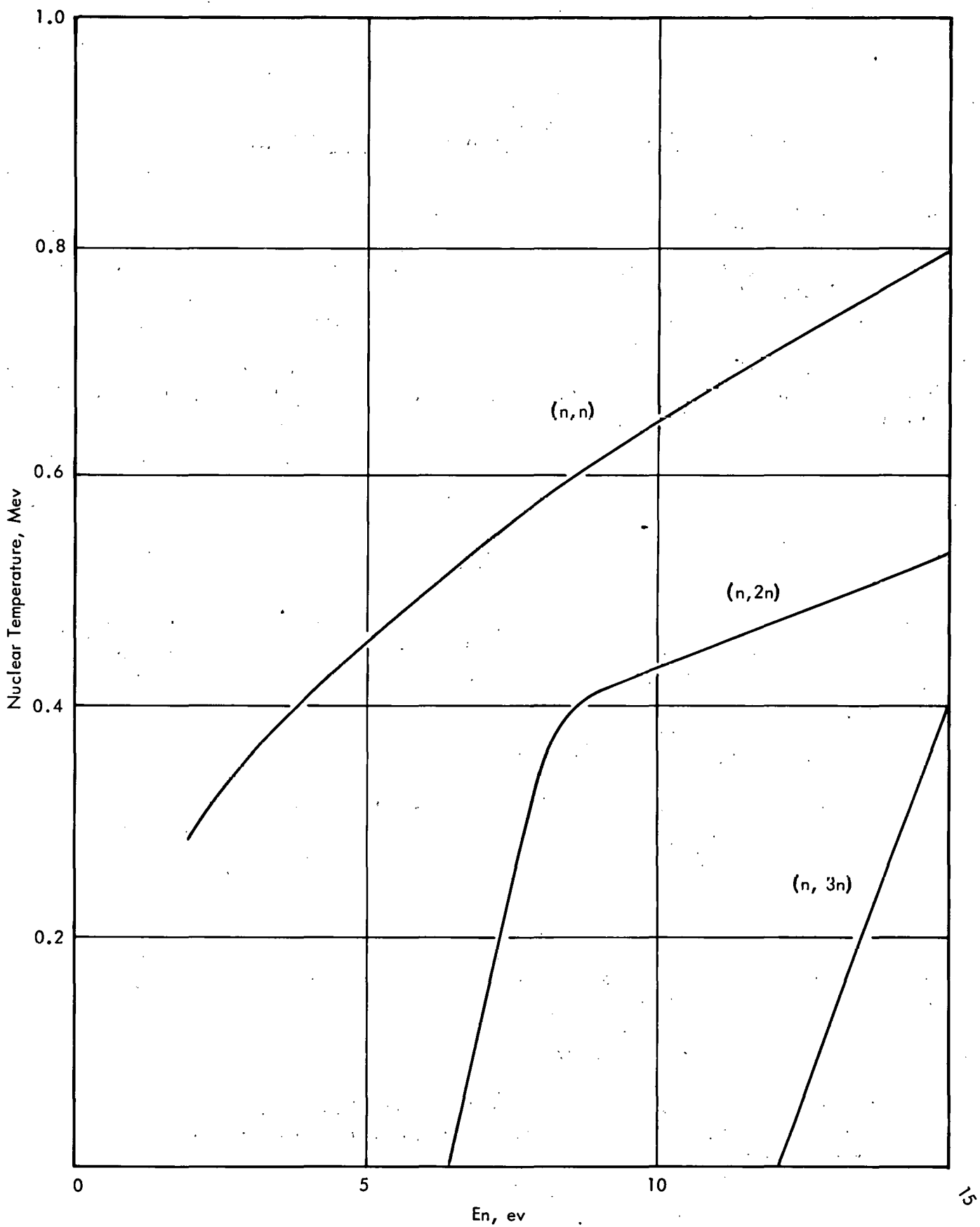
FIG. 20 NUCLEAR TEMPERATURES FOR INELASTIC SCATTERING, (N, 2N) AND (N, 3N) REACTIONS

C. SECONDARY ENERGY DISTRIBUTIONS (n, 2n) AND (n, 3n)

Present restrictions on ENDF/B data limit the choice of secondary energy distributions to a Maxwellian for (n, 2n) and (n, 3n) reactions. The work of LeCouteur[54] indicated that a reasonable approximation for the average energy of the emitted particles is

$$\overline{E} = 2\theta = \frac{4\theta_o}{3}$$

where θ_o is the temperature for the first neutron emitted. For neutron energies such that the excess energy above the threshold of 6.41 Mev is greater than the average energy obtained from this expression, $\theta = 2/3$, θ_o is used for the temperature where θ_o is is the inelastic scattering temperature.

For Pu-240, the excess neutron energy above the threshold is less than the above-defined average energy below 8 Mev. In the energy range between threshold and 8 Mev, it is assumed that the two neutrons share the available energy such that

$$2\theta = \overline{E} = \frac{E_n - E_{th}}{2} = \frac{E_n - 6.41}{2} \text{ Mev}$$

The threshold energy for the (n, 3n) reaction is 12.05 Mev. For this reaction, the nuclear temperature was determined by interpolating from approximately 0 at the threshold energy to a 15 Mev value estimated as 2/3 of the (n, 2n) temperature plus 1/3 of the inelastic scattering temperature evaluated at

$$E = 0.8 \ (15 - 12.05 - 4\theta_{n,2n})$$

The recommended temperatures are given in Figure 20.

THIS PAGE

WAS INTENTIONALLY

LEFT BLANK

V. COMPARISON WITH OTHER EVALUATIONS
AND RECENT MEASUREMENTS

A. COMPARISON WITH OTHER EVALUATIONS

1. Evaluation of Douglas

One of the most frequently used evaluations of Pu-240 cross sections for fast reactor analysis is that of Douglas,[45] which includes data above 1 kev, based on experimental data up to 1964. With the exception of capture cross sections, the present evaluation is in general agreement with the evaluation of Douglas. However, Douglas assumes the fission cross section to be zero below about 10 kev, while the present evaluation includes a recommended fission cross section over the entire energy range. Douglas' fission cross section sharply decreased from 0.062 barns at 40 kev to zero at about 10 kev. Between 40 kev and 200 kev, the Douglas fission cross section is about 30% smaller than the ENDF/B evaluation. These differences in the fission cross section below a few hundred kev are principally due to the p-wave fission analysis of this evaluation, which is based on experimental data since the previous evaluations. From 0.25 to 1 Mev, the fission cross sections in Douglas and ENDF/B evaluations are in good agreement. Above 1 Mev, the Douglas fission cross sections differ by about $\pm 5\%$ from ENDF/B values. This difference is due principally to renormalization of the experimental data in this evaluation. The Douglas evaluation for the Pu-240 capture cross section was based on a Pu-240/U-238 capture ratio of 1.75 and Parker's U-238 evaluation.[57] Above 10 kev, Douglas' capture cross section is about 50% larger than ENDF/B. This difference is primarily due to the difference in the estimation of the Pu-240/U-238 capture ratio between true evaluations. But, below 10 kev, differences in the reference U-238 capture cross section more than offset the differences in capture ratio; that is, between 6 and 10 kev, the Douglas cross section is 20% larger than ENDF/B; between 2 and 4 kev, it is 15% smaller than ENDF/B; and around 1 kev, it is again larger by 40% than ENDF/B.

2. Evaluation of Drake and Dyos

After Douglas' evaluation, GA evaluation of Pu-240 cross sections was made by Drake and Dyos.[56] Their evaluation is very similar to the Douglas evaluation above 1 kev but includes values down to thermal energies.

The recommended cross sections of Drake below a few ev are based on parameters for the 1 ev resonance. Drake chose $E_0 = 1.0575$ ev, $\Gamma_n = 2.46$ mv, $\Gamma_\gamma = 30$ mv, and $\Gamma_f = .0052$ mv for the parameters of the

49

first resonance which are to be compared with the ENDF/B values of Table III. Above this resonance, only parameters up to 120 ev were available at the time of Drake's evaluation. Drake assumed the fission width of the lowest resonance and the constant value of Γ_γ = 30 mv for all resolved resonances up to 120 ev, and the neutron widths have been taken directly from the recommended values of Hughes et al[58] except for the tenth level, for which the width has been taken from Fluharty and Simpson.[23]

In the unresolved region (120 ev to 1 kev), Drake used the average level spacing of 12 ev and s-wave strength function of 2.0×10^{-4} ev$^{-1/2}$ based on the Fluharty and Simpson[23] estimation. From the comparison of unresolved parameters between the Drake and ENDF/B evaluations (Γ_γ = 30 mv in both evaluations)

$$\frac{\langle\sigma_c\rangle^{Drake}}{\langle\sigma_c\rangle\,ENDF/B} \sim \frac{S^{Drake}}{S^{ENDF/B}} \frac{(\Gamma_\gamma + DS\sqrt{E})^{ENDF/B}}{(\Gamma_\gamma + DS\sqrt{E})^{Drake}} = \begin{cases} 1.5 \text{ at 1 kev} \\ 1.7 \text{ at 500 ev} \end{cases}$$

where S is the s-wave strength function and D is the average level spacing (below 1 kev, p-wave contribution is negligible). Drake's capture cross section is expected to be about 50% larger around 1 kev and 70% larger around 500 ev than ENDF/B data.

3. Evaluation of Davey

Recently Davey reported a re-evaluation of his previous study[33] for heavy isotope fission cross sections, which include Pu-240 fission cross section above 1 kev. Davey[59] normalized experimental data to his evaluated U-235 and Pu-239 fission cross sections described in the same report. His recommended fission ratio of Pu-240/U-235 is compared in Figure 7, where fairly large differences can be seen between the Davey and ENDF/B fission ratios of Pu-240/U-235 between 2.0 and 4.0 Mev. These differences are due principally to differences in the fission ratio of Pu-239/U-235 used to normalize Nesterov's data. In the ENDF/B evaluation, the Pu-239/U-235 ratio was obtained from the ratio of ENDF/B Pu-239 fission to Davey's[33] U-235 fission cross section. Between 2.0 and 4.0 Mev this ratio is larger than recommended by Davey in either of his evaluations. In Davey's latest evaluation, the greatest emphasis has been placed on the data of Perkin,[38] Gilboy,[35] Ruddick,[36] and White.[60] Davey's recommended cross section is roughly 10% smaller above 1.5 Mev than ENDF/B data.

The discrepancies in fission ratio, as indicated by this comparison of the ENDF/B and Davey evaluations, have resulted because the ENDF/B fission cross sections for nearly all isotopes were simultaneously and independently evaluated.

4. Evaluation of Yiftah

A recent evaluation of Pu-240 has been carried out by Yiftah[61] at the same time as this evaluation. Yiftah's evaluation is based on published measurements up to the time of the Paris Conference on Nuclear Data (October 1966), as is the ENDF/B evaluation. The comparisons of Yiftah's fission and capture cross sections with the present ENDF/B evaluation are given in Figure 21. The differences in fission cross sections above 10 kev are due principally to differences in normalization and interpolation through experimental data. Below 20 kev, Yiftah's data, strongly based on Byers' data,[30] are much greater than ENDF/B data. The differences in the capture cross section are due to the differences in unresolved resonance parameters. More detailed comparisons between the Yiftah and ENDF/B evaluations are given in Reference 62.

5. Modified ENDF/B

After the completion of the ENDF/B evaluation, the current authors made an alternate Pu-240 cross section evaluation, the details of which are given in References 62 and 63. In these references, calculations of the critical assemblies ZPR-III 48 and 48B are compared with integral measurements for both the ENDF/B and modified ENDF/B data files. The important differences in the Pu-240 cross sections between ENDF/B and modified ENDF/B are those in the capture and fission cross sections.

Comparison of the fission and capture cross sections of this evaluation with ENDF/B evaluation is given in Figure 21. The differences in fission cross section above a few hundred kev are due to differences in normalization. In this evaluation, the normalizations were made based on recent APDA U-235 and Pu-239 evaluations.[62] Below 10 kev, the modified ENDF/B fission cross section evaluation was based on the averaged data in Reference 31 and gives a larger fission cross section (a factor of 5 around 1 kev) than ENDF/B.

As seen in Figure 21, the modified ENDF/B capture cross section is 20 to 30% smaller than ENDF/B. This difference is due to the difference in the average radiation width. In modified ENDF/B, an average radiation width of 20 mv was used based on Asghar data,[6] while in ENDF/B evaluation, the value of 30 mv was used based on Bockhoff[5] and Byers.[7]

B. COMPARISON WITH RECENT DATA

Since the ENDF/B and modified ENDF/B evaluations of the present authors were completed, additional experimental data of Pu-240 resonance parameters were reported at the March 1968 Washington meeting on Neutron Cross Section and Technology. They are the measurements of the Central Bureau for Nuclear Measurements, EURATOM at Geel,[64] the detailed
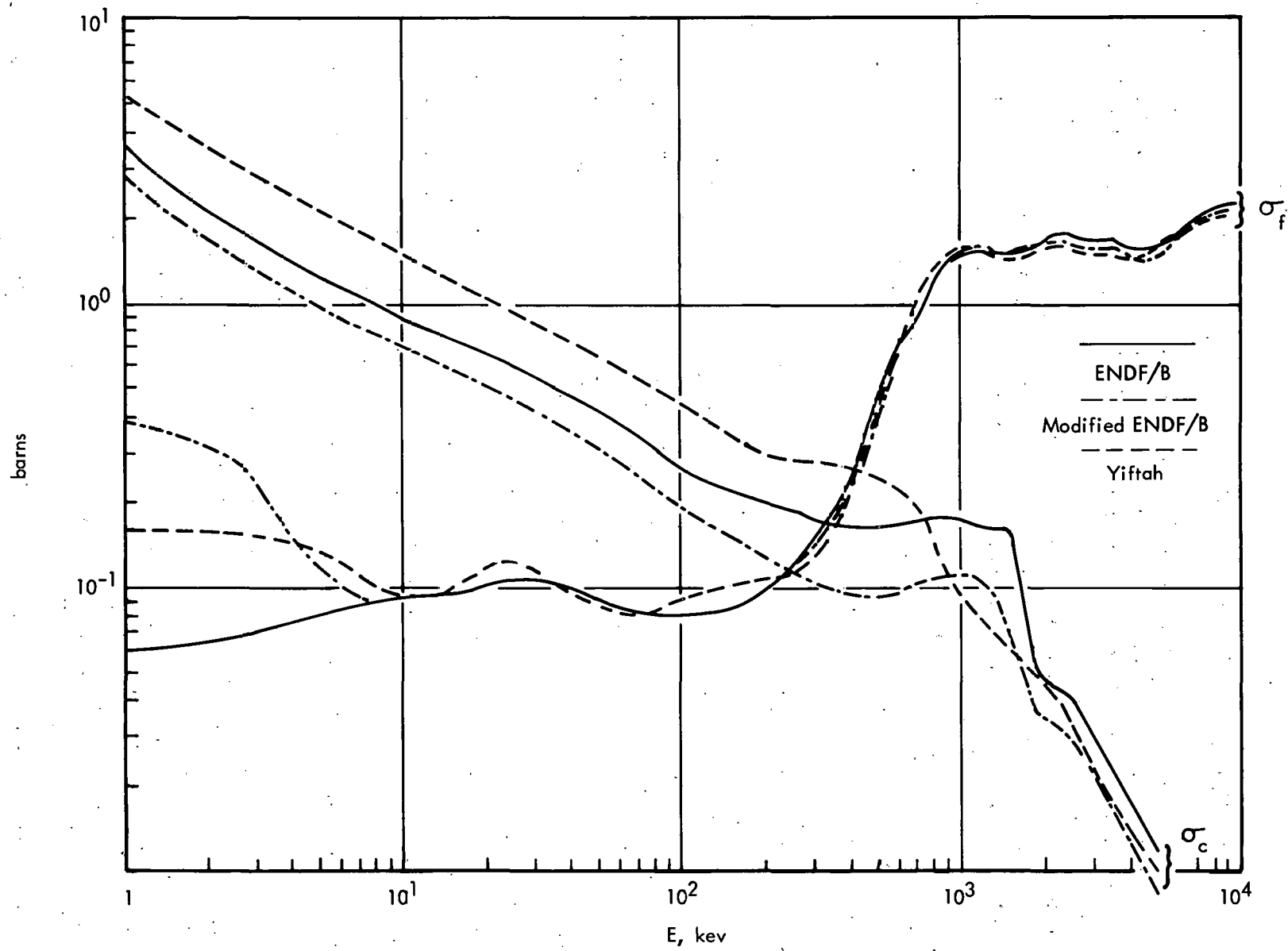
FIG. 21 FISSION AND CAPTURE CROSS SECTION OF Pu-240

information of which is not available at the time of this writing. According
to the abstract of that meeting,[64] however, they evaluated the full set of
resonance parameters E_r, Γ_n and Γ_γ between 38 ev and 820 ev by combin-
ing the results of the transmission experiments with those of a capture ex-
periment. They obtained the average radiation with $\langle \Gamma_\gamma \rangle$ = 23.2 $\pm$ 2.0 Mev.
For the 102 resonances up to 1500 ev, they obtained a mean level spacing of
$\langle D \rangle$ = 14.7 $\pm$ 0.8 ev and, presuming that all resonances in that range are
s-wave, an s-wave strength function of S_o = 1.05 $\pm$ 0.16 x 10^{-4} $ev^{-1/2}$ was
obtained. Their value of the average radiation width is between those of the
present ENDF/B and modified ENDF/B,[63] the mean level spacing is reason-
ably close to the ENDF/B value and the s-wave strength function is the same
as the ENDF/B estimation. To compare the APDA evaluations with these
data, average capture cross sections at typical energy points in the unre-
solved region using the above data have been calculated and compared with
ENDF/B and modified ENDF/B[63] values. The results are shown in Table
VII.

TABLE VII - COMPARISON OF THE EVALUATED CAPTURE
CROSS SECTIONS WITH RECENT DATA, BARNS

Energy, kev	ENDF/B	Modified ENDF/B	Geel Data with $S^{\ell=1}$ =1.75 x 10^{-4}
0.8	4.228	3.288	3.805
1.0	3.579	2.786	3.221
2.0	2.202	1.726	1.993
4.0	1.460	1.162	1.332
6.0	1.193	0.9534	1.090
8.0	1.045	0.8317	0.9549
10.0	0.9430	0.7557	0.8639
15.0	0.7966	0.6238	0.7226
20.0	0.6949	0.5425	0.6298
25.0	0.6255	0.4779	0.5598
30.0	0.5664	0.4318	0.5059
35.0	0.5209	0.3894	0.4608
40.0	0.4826	0.3574	0.4249

In the calculation with the Geel data, the same p-wave strength func-
tion of 1.75 x 10^{-4} $ev^{-1/2}$ as the ENDF/B evaluation was used.

The comparisons in Table VII show that the Geel data yield capture
cross sections which are between ENDF/B and modified ENDF/B values.
Using the Geel data with a p-wave strength function of 2.0 x 10^{-4} $ev^{-1/2}$, the
capture cross sections increase about 5% above 6 kev but remain between
ENDF/B and modified ENDF/B values.

THIS PAGE

WAS INTENTIONALLY

LEFT BLANK

REFERENCES

1. Stehn, J. R., et al, <u>Neutron Cross Sections</u>, BNL-325, 2nd ed. Supp. 2, Vol. 3, February 1965.

2. Pattendon, N. J., and Rainey, V. S., J. Nuclear Engineering, <u>11</u>, p. 14, 1959.

3. Leonard, B. R., "Nuclear Physics Research Quarterly Report for July-August-Sept.," HW-67219, 1960.

4. Moyer, W., et al, "Reports to the AEC Nuclear Cross Sections Advisory Group," WASH-1068, P/180, March 1966.

5. Bockhoff, K. H., et al, Paris Conference on Nuclear Data, 1966.

6. Asghar, M., Moxon, M. C., and Pattendon, N. J., ibid., CN-23/31.

7. Byers, D. H., et al, Conference on Neutron Cross Section Technology, Washington, D.C. (CONF-660303, 1966) and private communication.

8. Cote, R. E., et al, Phys. Rev., <u>114</u>, 505, 1959.

9. Egelstaff, D. B., et al, J. Nuc. Eng., <u>6</u>, 303, 1958.

10. Cornish, F. W., and Lounsbury, M., AECL-510, 1956.

11. Eroziellinsky, B. G., et al, J. Nuc. Eng., <u>4</u>, 86, 1957.

12. Kriepchinsky, A. P., J. Nuc. Eng., <u>6</u>, 155, 1957.

13. Rose, H. et al, Proc. of Second United Nations Conference on the Peaceful Uses of Atomic Energy, Geneva, P/14, 1958.

14. Walker, W. H., et al, Can. J. Phys., <u>38</u>, 57, 1960.

15. Nichols, P. F., "Effective Resonance Integral for Pu^{240} in Plutonium-Aluminum Alloy Rods," Nu. Sci. Eng., <u>17</u>, 144, 1963.

16. Walker, W. H., et al, "Proceedings of the International Conference and the Neutron Interactions with the Nucleus," USAEC Report TID-7547, 1957.

17. Egelstaff, P. A., et al, J. Nuc. Eng., <u>6</u>, 303, 1958.

18. Halperin, J., et al, J. Inorganic Chem., 9, 1, 1959.

19. Westcott, C., et al, Proc. of the Second United Nations on the Peaceful Uses of Atomic Energy, P/202, 1958.

20. Tattersall, R. B., AEEW-R115, 1962.

21. Bethe, H. A., Rev. Mod. Phys., 9, 69, 1937.

22. Newton, T. P., Can. J. Phys., 34, 804, 1956.

23. Simpson, O. D., and Fluharty, R. G., Bull. Am. Phy. Soc., 2, 219, 1957.

24. Schmidt, J. J., ANS National Topical Meeting, San Diego, Cal., February 1966.

25. Wittkopf, W. A., et al, "Neutron Cross Section Data," BAW-316, 1966.

26. Dunford, C. L., Private Communication.

27. Wheeler, J. A., Fast Neutron Physics, Part II, p 2051, 1963.

28. Patrick, B. H., and Pattenden, N. J., AERE-PR/NP7, 1964.

29. DeVroey, M., et al, Physics and Chemistry of Fission, Vol. 1 IAEA, 1965.

30. Byers, D. H., et al, American Physical Society Conference on Neutron Cross Section Technology, Washington, D.C., 1966.

31. "Fission Cross Section PETREL," LA-3586, Los Alamos Scientific Laboratory, December 1966.

32. Pitterle, T. A., and Green, D. M., "IDIOT, A Fortran V Code for Calculation of Resonance Averaged Effective Cross Sections and Their Temperature Derivatives," APDA-189, to be published.

33. Davey, W. G., "An Analysis of the Fission Cross Sections of ^{232}Th, ^{233}U, ^{234}U, ^{235}U, ^{236}U, ^{237}Np, ^{238}U, ^{239}Pu, ^{240}Pu, ^{241}Pu, and ^{242}Pu from 1 Kev to 10 Mev," Nuc. Sci. Eng., 26, pp 149-169, 1966.

34. White, P. H., J. Nucl. Energy, 19, 325, 1965.

35. Gilboy, W. B., et al, CN-23/7, 1966.

36. Ruddick, P. R., et al, J. Nuc. Eng., 18, 18, 1964.

37. DeVroey, M., et al, AERE-PR/NP7, 1964.

38. Perkin, J. L., et al, "The Fission Cross Sections of ^{233}U, ^{234}U, ^{235}U, ^{236}U, ^{237}U, ^{239}Pu, ^{240}Pu, and ^{241}Pu for 24 Kev Neutrons," J. Nucl. Energy, 19, 423-437, 1965.

39. Nesterov, V. G., and Smirenkin, G. N., Sov. J. Atm. En., 9, 511, 1960.

40. Greibler, P., et al, "Evaluation and Compilation of ^{239}Pu Cross Section Data for the ENDF/B Files," GEAP-5272, 1965.

41. Henkel, R. L., et al, AECD 4256, 1957.

42. Nesterov, B. G., and Smirenkin, G. N., Sov. Phy. JETP, 8, 367, 1959.

43. White, P. H., CNR/PR/6, 20, 1966.

44. Kazarinova, M. I., et al, Soviet J. Atm. En., 8, 125, 1961.

45. Douglas, A. C., AWREO-91/64, 1965.

46. Blatt, J. M., Weisskopf, V. F., Theoretical Nuclear Physics, John Wiley & Sons, New York, 1952.

47. Bethe, H. A., Physics Review, 50, 332, 1936; Rev. Mod. Phys., 9, 79, 1937.

48. DeVroey, M., et al, J. Nuc. Eng., 20, 191, 1965.

49. Kuzminov, B. D., "Soviet Progress in Neutron Physics," 1961.

50. Sanders, J. E., AERE R/M 169, Addendum, 1958.

51. Barton, D. M., et al, "Critical Masses of Composites of Oy and Pu-239-240 in Flat Top Geometry," Nu. Sci. Eng., 8, 543, 1960.

52. Engle, L. B., et al, Nuc. Sci. Eng., 8, 543, 1960.

53. Alter, H., Private Communication (to be published).

54. Terrell, J., Physics and Chemistry of Fission, Vol. 2, IAEA, 1965.

55. Pearlstein, S., et al, Private Communication.

56. Drake, M. K., Dyos, M. W., GA-6576, 1965.

57. Parker, K., AWRE Report No. 0-79/63, 1963.

58. Hughes, D. J., et al, BNL-325, 2nd ed., Supplement 1, 1960.

59. Davey, W. G., Nuc. Science Engr., $\underline{32}$, 35, 1968.

60. White, D. H., and Warner, G. P., J. Nuc. Eng., $\underline{21}$, 671, 1967.

61. Yiftah, S., et al, Symposium on Fast Reactor Physics and Related Safety Problems, SM-101/21, 1967.

62. Pitterle, T. A., et al, "A Comparison of Pu-240 Cross Section Evaluations by Calculations of ZPR-III Assemblies 48 and 48B," Second Conference on Nuclear Cross Sections and Technology, to be published.

63. Pitterle, et al, APDA-216, to be published.

64. Kolar, W., and Bockhoff, K. H., "Final Results of the Neutron Total Cross Section of Pu-240," Weigmann, H., et al, "Neutron Capture Measurements in the Resonance Region: Co and Pu-240," Abstract of Second Conference on Neutron Cross Sections and Technology, 1968.

65. LeConteur, K. J., Proc. Phys. Soc., A65, 718, 1952.

DISTRIBUTION LIST

USAEC - Chicago Operations Office
Director, Contracts Division (2)
G. H. Lee

USAEC - Washington, RDT
Director
Asst. Director, Program Management
Asst. Director, Reactor Engineering
Asst. Director, Reactor Technology
Asst. Director, Plant Engineering
Asst. Director, Nuclear Safety
Project Manager, LMEC
Project Manager, FFTF
Program Manager, LMFBR
Liquid Metal Projects Branch
Chem & Chem Separations Branch
Reactor Physics Branch
Fuels and Materials Branch
Applications and Facilities Branch
Components Branch
Instrumentation and Control Branch
Systems Engineering Branch
Core Design Branch
Fuel Handling Branch
Special Technology Branch
Reactor Vessels Branch

USAEC-RDT Site Representatives
Site Representative, APDA
Senior Site Representative, ANL
Senior Site Representative, AI
Acting Senior Site Representative, IdOO

USAEC-DTIE
R. L. Shannon (3)

USAEC - New York Operations Office
J. Dissler

USAEC - San Francisco Operations Office
J. Holliday

Director, LMFBR Program Office, ANL
A. Amorosi

Director, LMEC, AI
R. W. Dickinson

Aerojet - General Corporation
H. Derow

Argonne National Laboratory
R. Bane
L. W. Fromm
S. Greenberg
L. J. Koch
S. Lawroski
M. Novick
F. Smith

Atomics International
R. Balent (2)
S. Golan

Babcock & Wilcox Company
(Box 1260, Lynchburg, Va 24505)
M. W. Croft

Babcock & Wilcox Company
(Barberton, Ohio)
P. B. Probert

Baldwin-Lima-Hamilton Corp.
(Industrial Equipment Div., Eddystone, Pa)
J. G. Gaydos
R. A. Tidball

Brookhaven National Laboratory
O. E. Dwyer
D. Gurinsky (2)
K. Hoffman
C. Klamut
L. Newman
A. Romano

Combustion Engineering, Inc.
(Box 500, Windsor, Conn)
W. P. Staker
W. H. Zinn

General Electric Company
(175 Curtner, San Jose, Calif 93125)
K. P. Cohen (3)

General Electric Company
(310 DeGuigne, Sunnyvale, Calif 94086)
A. Gibson

Gulf General Atomic, Div. of Gulf Oil Co.
(San Diego, California)
P. Fortescue

M. W. Kellogg Company
(711 Third, New York, New York)
E. W. Jesser

Lewis Flight Prop. Laboratory, NASA
(21000 Brookpark, Cleveland, Ohio)
C. A. Barrett

Los Alamos Scientific Laboratory
D. B. Hall (2)
G. Waterbury
W. R. Wykoff

MSA Research Corporation
(Callery, Pa 14024)
C. H. Staub

Nuclear Materials & Equipment Corp.
(Apollo, Pennsylvania)
   Z. M. Shapiro

Oak Ridge National Laboratory
(Box X, Oak Ridge, Tennessee)
    F. L. Culler (2)
    J. H. Devan
    D. Gardiner
    J. White

Oak Ridge National Laboratory
(Box Y, Oak Ridge, Tennessee)
   R. E. MacPherson, Jr.

Pacific Northwest Laboratory, BMI
    E. Astley (5)

Power Reactor Development Company
(1911 First, Detroit, Michigan 48226)
    A. S. Griswold

Southwest Atomic Energy Associates
(Box 1106, Shreveport, La 71102
   J. R. Welsh

United Nuclear Corporation
(Box 1583, New Haven, Conn)
    A. Strasser (2)

Westinghouse Electric Corporation
(Box 158, Madison, Pa 15663)
   J. C. R. Kelly, Jr. (2)

Westinghouse Electric Corporation
(Box 158, Madison, Pa 15663)
    C. A. Anderson

Westinghouse Electric Corporation
(Westinghouse Research Laboratories
 Churchill Borough, Pittsburgh,
 Pennsylvania 15235)
    E. Berky

USAEC-UKAEA Exchange
UKAEA
Reactor Group Headquarters
Risley, Warrington, Lancashire
England
    J. Stephenson (12)

USAEC-EURATOM Exchange
EURATOM
53, Rue Belliard
Brussels 4, Belgium
    A. deStordeur (10)

CNEN
Via Mazzini 2
Bologna, Italy
    F. Pierantoni (4)

CEN Saclay
Boite Postale 2
Gif-Sur-Yvette (Set 0) France
    G. Vendryes (10)

Kernforschungszentrum Karlsruhe
7500 Karlsruhe, Germany
    W. Haefele (10)